THE JOURNAL OF BIOLOGICAL CHEMISTRY VOL. 286, NO. 1, pp. 687–706, January 7, 2011

Kallikrein-related Peptidase-8 (KLK8) Is an Active Serine Protease in Human Epidermis and Sweat and Is Involved in a Skin Barrier Proteolytic Cascade[S]

Received for publication, March 22, 2010, and in revised form, September 30, 2010 Published, JBC Papers in Press, October 12, 2010, DOI 10.1074/jbc.M110.125310

Azza Eissa[‡§], **Vanessa Amodeo**[§], **Christopher R. Smith**[¶], **and Eleftherios P. Diamandis**[‡§¶1]

From the [‡]*Department of Laboratory Medicine and Pathobiology, University of Toronto, Toronto, Ontario M5S 1A8, the* [§]*Department of Pathology and Laboratory Medicine, Mount Sinai Hospital, Toronto, Ontario M5T 3L9, and the* [¶]*Department of Clinical Biochemistry, University Health Network, Toronto, Ontario M5G 1X5, Canada*

Kallikrein-related peptidase-8 (KLK8) is a relatively uncharacterized epidermal protease. Although proposed to regulate skin-barrier desquamation and recovery, the catalytic activity of KLK8 was never demonstrated in human epidermis, and its regulators and targets remain unknown. Herein, we elucidated for the first time KLK8 activity in human non-palmoplantar stratum corneum and sweat *ex vivo*. The majority of stratum corneum and sweat KLK8 was catalytically active, displaying optimal activity at pH 8.5 and considerable activity at pH 5. We also showed that KLK8 is a keratinocyte-specific protease, not secreted by human melanocytes or dermal fibroblasts. KLK8 secretion increased significantly upon calcium induction of terminal keratinocyte differentiation, suggesting an active role for this protease in upper epidermis. Potential activators, regulators, and targets of KLK8 activity were identified by *in vitro* kinetic assays using pro-KLK8 and mature KLK8 recombinant proteins produced in *Pichia pastoris*. Mature KLK8 activity was enhanced by calcium and magnesium ions and attenuated by zinc ions and by autocleavage after Arg^{164}. Upon screening KLK8 cleavage of a library of FRET-quenched peptides, trypsin-like specificity was observed with the highest preference for (R/K)(S/T)(A/V) at P1-P1′-P2′. We also demonstrated that KLK5 and lysyl endopeptidase activate latent pro-KLK8, whereas active KLK8 targets pro-KLK11, pro-KLK1, and LL-37 antimicrobial peptide activation *in vitro*. Together, our data identify KLK8 as a new active serine protease in human stratum corneum and sweat, and we propose regulators and targets that augment its involvement in a skin barrier proteolytic cascade. The implications of KLK8 elevation and hyperactivity in desquamatory and inflammatory skin disease conditions remain to be studied.

The first line of defense for skin against chemical, physical, and microbial insults is its outermost epidermal layer, the stratum corneum (SC).[2] The SC is continuously produced through terminal differentiation of keratinocyte cells in lower epidermal layers, which is paralleled by the simultaneous shedding of superficial cells known as corneocytes from the surface. Although the SC is composed of flattened corneocytes, which are incapable of synthesizing new proteins, its extracellular environment is an active hub for different metabolic activities regulating various skin barrier functions (1, 2). Among the key SC extracellular molecules are a group of proteolytic enzymes known as kallikrein-related peptidases.

The human kallikrein-related peptidase family (KLKs) is composed of 14 serine proteases (KLK2 to KLK15) that share a similar homology to the parent human tissue kallikrein (KLK1) (3–5). KLK transcripts are encoded by a multigene cluster on chromosome 19q13.4 and are translated as prepropeptide single chains. They are secreted as latent zymogens, which are activated after cleavage of their propeptide. To date, SC serine peptidase activity is mainly attributed to KLK5, KLK7, and KLK14, which were originally identified in SC tissues in both active and inactive forms (6–8). These KLKs function as desquamatory enzymes by cleaving corneodesmosomal adhesion molecules in the SC, leading to regulated corneocyte shedding (7, 9, 10). Active epidermal KLKs are proposed to function through an orchestrated proteolytic cascade in the skin, which regulates their zymogen activation and targeting of corneodesmosome degradation (11–13) and antimicrobial peptide activation during infection (14), thus allowing these processes to occur only when physiologically required. In this proteolytic activation cascade, KLK5 autoactivates and then activates pro-KLK7 and pro-KLK14, and the activated KLK14 activates pro-KLK5 forming a positive feedback loop. The inherent pH and calcium ion gradients in the stratum corneum, as well as changes induced by trauma to the skin barrier, have been suggested to trigger and/or regulate this activation cascade. Aberrant KLK cascade activities are implicated in skin diseases characterized by abnormal barrier functions, such as psoriasis vulgaris (15), acne rosacea (16), atopic dermatitis (17), and Netherton syndrome (18, 19).

We recently showed that additional trypsin-like KLK peptidases, including KLK6, KLK8, KLK10, KLK11, and KLK13, co-exist with KLK5, KLK7, and KLK14 in stratum corneum

[S] The on-line version of this article (available at http://www.jbc.org) contains supplemental Tables 1–3 and Figs. 1–6.

[1] To whom correspondence should be addressed: Mount Sinai Hospital, Joseph and Wolf Lebovic Centre, 6th Fl., Rm. 6-201, 60 Murray St., Toronto, Ontario M5T 3L9, Canada. Tel.: 416- 856-8443; Fax: 416-619-5521; E-mail: ediamandis@mtsinai.on.ca.

[2] The abbreviations used are: SC, stratum corneum; KLK, kallikrein-related peptidase; AMC, 7-amino-4-methylcoumarin; SLPI, secretory leukocyte protease inhibitor; LEKTI, lymphoepithelial Kazal-type inhibitor; AP, antimicrobial peptide; BisTris, 2-[bis(2-hydroxyethyl)amino]-2-(hydroxymethyl)propane-1,3-diol; mat, mature form; AT, α1-antitrypsin; PNGase, peptide *N*-glycosidase.

tissues, hair follicles, and sebaceous and sweat glands (20, 21). Interestingly, we found KLK8 to be the most abundant trypsin-like KLK in normal stratum corneum and sweat, among the seven KLKs tested (21). Human KLK8 was originally cloned from skin cDNA as the homologue of mouse neuropsin, as its cDNA and predicted amino acid sequence have 72% identity to mouse neuropsin (22). Although neuropsin mRNA and protein are detected in high amounts in mouse brain and skin tissues (23, 24), KLK8 protein was not detected in human brain tissues. Work done in Klk8/neuropsin-null mice suggested that Klk8/neuropsin is involved in skin barrier homeostasis, whereby healing of chemically wounded or UV-irradiated mouse skin is largely impaired in its absence (25, 26). Additionally, the dramatic increase of KLK8 mRNA in hyperkeratotic skin of psoriasis vulgaris, seborrheic keratosis, lichen planus, and squamous cell carcinoma patients, compared with normal and basal cell carcinoma skin, suggested that human KLK8 is involved in keratinocyte differentiation and skin barrier formation (27). We also detected KLK8 protein overexpression in psoriasis, atopic dermatitis, and peeling skin syndrome skin tissues (15, 17, 28). Thus, KLK8 involvement in normal skin barrier formation and inflammatory skin disease pathology has recently become apparent.

Despite the recent progress in detecting KLK8 expression in normal skin and skin pathologies, KLK8 enzymatic regulation and activity in normal skin remain to be investigated. It is essential to probe KLK8 protease activity in normal skin, in addition to continuing the ongoing investigation of KLK8 function and regulation in Klk8/neuropsin knock-out mouse skin. This must be done while keeping in mind the anatomical and physiological differences between mouse and human skin, as well as differences at the molecular level. For instance, KLK5 is not detected in mouse skin (29), although it is a significant active protease in human stratum corneum and a major player in the desquamation cascade in normal skin physiology. Also, the activation motif of human KLK8 (QEDK-VLGGH) differs from that of the mouse Klk8/neuropsin (QGSK-ILEGR), suggesting that endogenous activators of KLK8 may differ between mouse and human species, even though these proteases may play similar roles.

To investigate human KLK8 enzymatic properties and delineate its potential activators and downstream targets in normal skin, we produced recombinant human KLK8 in its latent zymogen (pro-KLK8) and active mature form (mat-KLK8) in yeast *Pichia pastoris* for *in vitro* activation and degradation assays. Recombinant KLK8 regulation by relevant epidermal pH and cations, potential epidermal activators, and inhibitors was investigated in a series of enzymatic assays. We also examined recombinant mat-KLK8 substrate specificity via kinetic analysis of its cleavage of a panel of fluorogenic AMC substrates and a small position-scanning library of internally quenched FRET peptides. The ability of KLK8 to activate potential co-localized epidermal pro-KLKs and LL-37 antimicrobial peptide was also examined. We performed these *in vitro* biochemical characterization assays under the hypothesis that this protease is induced during terminal keratinocyte differentiation and is activated in the SC extracellular space to participate in barrier functions. Thus, we suspected that this serine protease is active in normal upper epidermis and sweat. Herein, we investigated KLK8 expression during terminal keratinocyte differentiation in culture and developed a sensitive and specific immunocapture assay to probe its activity in human epidermal extracts and sweat *ex vivo*. Our findings shed light on the orphan epidermal protease KLK8 and provide evidence that this KLK is indeed an active serine protease in human stratum corneum and sweat and is an intriguing member of a proteolytic cascade regulating skin barrier integrity.

EXPERIMENTAL PROCEDURES

Materials

The rapid endoprotease profiling library of fluorescence resonance energy transfer (FRET) quenched peptides (PepSets™REPLi) was purchased from Mimotopes Pty Ltd. (Australia). The human antimicrobial LL-37 peptide (Leu-Leu-Gly-Asp-Phe-Phe-Arg-Lys-Ser-Lys-Glu-Lys-Ile-Gly-Lys-Glu-Phe-Lys-Arg-Ile-Val-Gln-Arg-Ile-Lys-Asp-Phe-Leu-Arg-Asn-Leu-Val-Pro-Arg-Thr-Glu-Ser) was purchased from Genemide Synthesis, Inc. (San Antonio, TX). The majority of synthetic fluorogenic AMC substrates was purchased from Bachem Bioscience (King of Prussia, PA). AAPF-AMC and AAPV-AMC were obtained from Calbiochem. All AMC substrates were diluted in DMSO at a final concentration of 80 mM and stored at −20 °C. Recombinant KLK5 and KLK14 were produced in *P. pastoris* as described previously (30, 31). Recombinant pro-KLC1 was produced in Chinese hamster ovary cells, and recombinant pro-KLK1 was produced in the human embryonic kidney cell line, HEK293, as described previously (32, 33). LEKTI fragments containing intact domains 1–6, LEKTI(1–6), domains 6–8 and partial domain 9, LEKTI(6–9′), domains 9–12, LEKTI(9–12), and domains 12–15, LEKTI(12–15), were produced in a baculovirus/insect system as reported previously (34, 35). Recombinant SLPI, neutrophil elastase, and elafin were purchased from R & D Systems Inc. (Minneapolis, MN), Calbiochem, and Sigma, respectively, and diluted to a final concentration of 0.5g/liter and stored at −80 °C.

Cloning, Expression, and Purification of Recombinant Human KLK8 Proteins

Active Mat-KLK8—Recombinant mat-KLK8 protease was produced in the *original P. pastoris* expression system (Invitrogen). Briefly, PCR-amplified DNA fragment encoding mature KLK8 isoform-1 (amino acids 33–260 of NCBI GenBank™ accession number NP_009127) flanked by XhoI and EcoRI restriction enzyme sites was cloned into pPIC9 expression vector, in-frame with its α-secretion signal and the alcohol oxidase *AOX1* gene. Purified mat-KLK8-pPIC9 DNA construct was confirmed by sequencing using 5′-*AOX1*, 3′-*AOX1*, and α-secretion signal vector-specific primers and NCBI BLAST Align program. For details on primer sequences used for cloning, please refer to supplemental Fig. 1 and Table 1. The mat-KLK8-pPIC9 construct was linearized with SacI and transformed into KM71 *P. pastoris* strain by electroporation. A stable KM71 transformant was grown in 1 liter of BMGY media. After 2 days, yeast culture was centrifuged, and the cell pellet was resuspended in 300 ml of BMMY media

(A_{600} = 10). Recombinant KLK8 expression was induced with 1% methanol for 5 days at 30 °C in a shaking incubator (250 rpm). Recombinant mat-KLK8 was purified from culture supernatant by ultraconcentration, serial dialysis, and centrifugation procedures, followed by cation-exchange chromatography. One liter of culture containing secreted mat-KLK8 was centrifuged, and the supernatant was concentrated 10-fold by positive pressure ultracentrifugation in an Amicon™ stirring chamber (Millipore Corp., Bedford, MA) with a 10-kDa cutoff regenerated cellulose membrane (Millipore). A series of bench-top purification experiments using an aliquot of KLK8-containing supernatant and SP-Sepharose Fast Flow beads packed in Econo-Pac open column (Bio-Rad) were performed. We determined the optimal binding buffer for cation-exchange purification of mat-KLK8 to be 0.01 M acetic acid containing 50 mM NaCl, pH 4.76, and the optimal salt concentration for elution to be 250 mM NaCl. These findings were translated into an automated method where mat-KLK8 protein was purified using an automated ÄKTA FPLC system on a pre-equilibrated 5-ml cation-exchange HiTrap high performance Sepharose HP-SP column (GE Healthcare), after serial dialysis (three times) against 0.01 M acetic acid, 50 mM NaCl, pH 4.76, running buffer A. Mat-KLK8 was eluted in 4-ml fractions via a stepwise salt gradient using 1 M NaCl in 0.01 M acetic acid, pH 4.76, buffer B, at a flow rate of 1 ml/min, as follows: (*a*) 5% B for 25 min; (*b*) 10% B for 25 min; (*c*) 15% for 25 min; (*d*) 25% for 15 min; and (*e*) followed by a continuous gradient from 25 to 100% B for 15 min. Recombinant mat-KLK8 was further purified using a 10-ml cation-exchange Source15S Tricorn™ column (GE Healthcare), which resulted in elution of a very pure protein in three fractions that were pooled, concentrated, and stored at −80 °C.

Pro-KLK8 Zymogen—Pro-KLK8 isoform-1 cDNA (amino acids 29–260) was cloned into pPIC9 *P. pastoris* yeast vector and transformed into a stable GS115 yeast strain as described above for mat-KLK8. The recombinant colony was grown in 1 liter of BMGY medium for 1 day and resuspended in 2 liters of BMMY (A_{600} = 1.0). Pro-KLK8 expression was induced with 1% methanol for 6 days at 30 °C in a shaking incubator (250 rpm). After concentrating the culture supernatant 20-fold, recombinant pro-KLK8 was purified after serial dialysis by cation-exchange chromatography using a HiTrap high performance Sepharose HP-SP column connected to an automated ÄKTA FPLC system. Pro-KLK8 was eluted in 4-ml fractions using the same step gradient described above for mat-KLK8 purification. A second purification step was performed, where FPLC fractions containing pro-KLK8 were pooled and loaded onto a Superdex 200 HR10/30 gel filtration column (GE Healthcare). The protein eluted as a single peak, and the protein-containing fractions were pooled, concentrated, and stored at −80 °C. For both recombinant mature and pro-KLK8 proteins, purity was assessed on silver-stained SDS-PAGE (described below). Concentration was determined by the BCA method (Pierce), and protein identity was confirmed by mass spectrometry and N-terminal sequencing. Protein aliquots were stored at −80 °C in their elution buffer, 0.01 M acetic acid containing 250 mM NaCl, pH 4.76.

Detection of Recombinant Mat-KLK8 and Pro-KLK8 Protein Expression

SDS-PAGE—SDS-PAGE was performed using the NuPAGE BisTris electrophoresis system and precise 4–12% gradient polyacrylamide gels at 200 V for 45 min (Invitrogen). Proteins were visualized with a Coomassie G-250 staining solution, SimplyBlue™ SafeStain (Invitrogen), and/or by silver staining with the Silver Xpress™ kit (Invitrogen), according to manufacturers' instructions.

Western Blotting—For immunoblotting of KLK8, proteins resolved by SDS-PAGE were transferred onto a Hybond-C Extra nitrocellulose membrane (GE Healthcare) at 30 V for 1 h. The membrane was blocked with Tris-buffered saline/Tween (0.1 mol/liter Tris-HCl buffer, pH 7.5, containing 0.15 mol/liter NaCl and 0.1% Tween 20) supplemented with 5% nonfat dry milk overnight at 4 °C and probed with a KLK8 polyclonal rabbit antibody (produced in-house; diluted 1:2000 in Tris-buffered saline/Tween) for 1 h at room temperature. The membrane was washed three times for 15 min with Tris-buffered saline/Tween and treated with alkaline phosphatase-conjugated goat anti-rabbit antibody (1:5000 in Tris-buffered saline/Tween; Jackson ImmunoResearch) for 1 h at room temperature. Finally, the membranes were washed again as above, and the signal was detected on x-ray film using chemiluminescent substrate (Diagnostic Products Corp., Los Angeles).

Mass Spectrometry and N-terminal Sequencing—Mass spectrometry analysis for positive identification of both recombinant pro- and mat-KLK8 proteins was performed. N-terminal sequencing was performed by the Edman degradation method. Briefly, proteins were transferred by electroblotting to polyvinylidene difluoride membrane and visualized with Coomassie Blue Stain. The bands were excised and applied to the sequencer.

Glycosylation Status—Denatured KLK8 in 5% SDS, 0.4 M DTT was incubated with peptide *N*-glycosidase (PNGase F) (New England Biolabs) in 0.5 M sodium phosphate, pH 7.5, and 10% Nonidet P-40 surfactant. The mixture was incubated at 37 °C for 3 h. Deglycosylated KLK8 as well as mock-treated KLK8 containing no PNGase F were subjected to SDS-PAGE and stained with SimplyBlue™ SafeStain (Invitrogen). Glycosylation analysis was also repeated without the denaturation step to test deglycosylation effect on mat-KLK8 activity.

Recombinant Mat-KLK8 Activity and Substrate Specificity

Gelatin Zymography—Mat-KLK8 proteolytic activity was visualized by gelatin zymography (Novex® 10% Zymogram, gelatin, Invitrogen), according to the manufacturer's instructions. Briefly, mat-KLK8 was diluted 1:1 in Tris-glycine SDS sample buffer and electrophoresed for 2 h at 125 V at 4 °C. After electrophoresis, the gels were incubated in renaturing buffer for two 30-min intervals at room temperature, followed by incubation in developing buffer for 4 h at 37 °C. Gels were stained with SimplyBlue™ SafeStain and destained until the white lytic bands corresponding to areas of protease activity were visible against a dark blue background.

Fluorogenic AMC Substrate Profiling and Kinetics Constant Determination—Mat-KLK8 hydrolysis of 16 fluorogenic AMC peptides was investigated using the same KLK8 concentration (12 nM) and increasing concentrations of AMC peptides (0.03, 0.06, 0.12, 0.25, 0.50, 0.75, and 1.0 mM) in KLK8 activity buffer (100 mM phosphate, 0.01% Tween 20, pH 8.5). The trypsin-like substrate peptides tested were VPR-AMC, GGR-AMC, FSR-AMC, PFR-AMC, LKR-AMC, LRR-AMC, QRR-AMC, QAR-AMC, QGR-AMC, GPR-AMC, GPK-AMC, EKK-AMC, and LK-AMC. AAPF-AMC and LLVY-AMC were the chymotrypsin-like substrate peptides tested. The known neutrophil elastase substrate AAPV-AMC was used as a negative control. KLK8-free reactions, for each peptide concentration, were used as negative controls, and background counts were subtracted from each value. Free AMC fluorescence was measured on the Wallac 1420 Victor^{2TM} fluorometer (PerkinElmer Life Science) with excitation and emission filters set at 380 and 480 nm, respectively, at 1-min intervals for 20 min at 37 °C. A standard curve was constructed using known concentrations of AMC to calculate the rate of free AMC emission. The slope of the resultant AMC standard curve was 19.18 AMC fluorescence counts/nM free AMC. The steady-state (Michaelis-Menten) kinetic constants (k_{cat}/K_m) were then calculated by nonlinear regression analysis using Enzyme Kinetics Module 1.1 (Sigma Plot, SSPS, Chicago). All experiments were performed in triplicate and repeated at least twice.

KLK8 Cleavage of a Position-scanning Rapid Endopeptidase Library (RepLi) of FRET-quenched Peptides—The RepLi library contains FRET-quenched peptide pools lyophilized into 512 wells in a total of six 96-well plate format. Each well contains eight peptides with the same amino acid combinations in their variable tri-peptide core, which allows screening of 512 peptide pools with 3375 potential cleavage sites. The soluble peptide library pools (*i.e.* 512 wells) in six 96-well plates were diluted with mat-KLK8 activity buffer, 100 mM sodium phosphate buffer without Tween 20, pH 8.50, to a final concentration of 50 μM. Tween 20 was not included because it is not compatible with mass spectrometry analysis. After agitating the plate for 1 min, 20-μl aliquots of each well were collected as background controls. Background readings were measured using Envision 2103 Multilabel Reader (excitation $\lambda = 320$ nm, emission $\lambda = 400$ nm). After measuring background readings, 10 μl of mat-KLK8 was added (10 nM final) to each well of the six 96-well RepLi plates, prior to incubating plates at 37 °C for 1 h. This library was incubated with a minimal amount of active enzyme (10 nM) for 1 h to avoid selection of peptides containing nonoptimal cleavage sites. Fluorescence data were analyzed before and after protease addition. Cleavage was determined by assigning "strong, moderate, weak, and no cleavage" identifiers to wells generating a signal to background ratio (S:B) of "≥2, between 1.50 and 2.0, between 1.25 and 1.50, and ≤1.25," respectively. The cleavage sites of selected wells that showed the highest fluorescence readings were determined by LC-MS analysis, comparing the sample before and after mat-KLK8 addition.

Regulation of KLK8 Activity

pH Profiling, Divalent Cation, and Glycosylation Effect on Mat-KLK8 Activity—Four buffer systems were assessed to determine the optimal pH for mat-KLK8 activity; 1 M potassium phosphate buffer (pH 5.0–6.5), PBS (pH 7.0–7.5), 50 mM Tris-HCl (pH 8.0–9.0), and 100 mM sodium phosphate (pH 7.0–9.0). Solutions prepared from salts of $ZnCl_2$, $MgCl_2$, $CaCl_2$, NaCl, and KCl were added to optimal activity buffer containing 0.25 mM VPR-AMC at a final concentration of (0, 10^{-2}, 10^{-3}, 10^{-4}, 10^{-5}, 10^{-6}, and 10^{-7} nM) in a final volume of 100 μl. At this point, KLK8 (12 nM) was applied to each reaction mixture, and the plate was agitated for 1 min. Residual KLK8 activity against VPR-AMC after incubation in each buffer pH or with each individual cation was calculated. Alternatively, mat-KLK8 was treated with PNGase F to remove *N*-glycans without denaturation. The same amount of PNGase-treated mat-KLK8 and mock-treated mat-KLK8 (12 nM) was added to activity buffer containing VPR-AMC (0.25 mM) in a final volume of 100 μl, and AMC fluorescence was measured to test the deglycosylation effect on KLK8 activity.

Mat-KLK8 Autodegradation—Aliquots of intact mat-KLK8 enzyme (100 ng) were incubated in KLK8 activity buffer at 4, 25, and 37 °C for 0, 0.5, 1, 2, 4, 6, 12, 24, and 34 h. Autodegradation fragments were detected by reduced silver-stained SDS-PAGE, and their activity was tested against VPR-AMC substrate, as described above.

Pro-KLK8 Activation by Active KLK5, KLK1, and Lysyl Endopeptidase—Activation studies of pro-KLK8 by potential recombinant activators were done in two consecutive steps, an "activation step" followed by a "detection step." In the activation step by mat-KLK5, pro-KLK8 (200 nM) was added to 20 nM active KLK5 at increasing incubation times at 37 °C (1, 3, 18, 24, and 48 h) and at 25 °C (day 1, 2, and 4) in KLK5-optimized activity assay buffer (100 mM phosphate buffer, 0.01% Tween 20, pH 8.0) in a total volume of 35 μl. In the detection step, pro-KLK8 activation was monitored as an increase in the fluorescence of cleaved AMC, off VPR-AMC, after adding 10 μl of the activation mix to 90 μl of KLK8-optimized assay buffer (100 mM phosphate buffer, 0.01% Tween 20, pH 8.5) containing 0.1 mM VPR-AMC. To avoid confounding results due to KLK5 similar activity toward VPR-AMC, we included a duplicate activation mix where α_1-antitrypsin inhibitor (AT) is added to quench KLK5 activity prior to detecting pro-KLK8 activation. AT was added at a 5-fold molar excess and incubated for an additional hour at 37 °C. Activity toward VPR-AMC was measured for both reaction mixtures, with or without AT in triplicate. To test activation of pro-KLK8 by KLK1, 200 nM pro-KLK8 was incubated with 20 nM active mat-KLK1 for 1 and 3 h at 37 °C in 35 μl of activity assay buffer (100 mM phosphate buffer, 0.01% Tween 20, pH 8.0). Pro-KLK8 activation by lysyl endopeptidase was performed by incubating 200 nM pro-KLK8 with lysyl endopeptidase in its optimal activity buffer (50 mM Tris, 10 mM $CaCl_2$, 150 mM NaCl, pH 9.0) at an activator to pro-KLK8 molar ratio of 1:1000 for 1 h at 37 °C in a 35-μl total volume. "Detection" of activation was done in triplicate where 10 μl of each activation mix was added to 90 μl of KLK8-optimized assay buffer (100 mM phosphate buffer,

0.01% Tween 20, pH 8.5) containing 0.1 mM VPR-AMC. The fluorescence values obtained for the activation mix, pro-KLK8 alone, and activator alone reaction controls were subtracted from raw values of the no enzyme background control. The reaction rate was then calculated by measuring the slope in fluorescence units/min and converting it to free AMC (nM)/min.

Mat-KLK8 Inhibition by Epidermal Inhibitors and General Serine Protease Inhibitors—Mat-KLK8 (12 and 3 nM) was incubated with 30 nM of each of the four LEKTI domains (D1–6, D6–9, D9–12, and D12–15) for 1 h at 37 °C in optimal KLK8 activity buffer. To detect the potential inhibitory effect of each LEKTI fragment, 10 μl of each mix was added to 90 μl of KLK8-optimized assay buffer containing 0.25 mM VPR-AMC. 12 nM of KLK5 was also incubated with each inhibitory LEKTI fragment as a positive control. SLPI or elafin (60 nM and 600 nM) were incubated separately with mat-KLK8 (6 nM) in a final volume of 20 μl for 1 h at 37 °C. Control reactions, *i.e.* elastase, elafin, and SLPI incubated alone, were also performed. 6 nM neutrophil elastase was tested as a positive control for SLPI and elafin inhibition. KLK8 activity was also tested upon incubating with 0.1 or 0.01 mg/ml soybean trypsin inhibitor or aprotinin, 1 mM PMSF, 1 mg/ml α_1-antitrypsin inhibitor, and 1 mg/ml chymostatin for 1 h at 37 °C in optimal KLK8 activity buffer. 10-μl aliquots of each inhibitor-treated and nontreated reaction mix were added to 90 μl of KLK8-optimized assay buffer containing 0.25 mM VPR-AMC in triplicate in a 96-well plate, so that the final KLK8 concentration in each well is 6 nM. Enzyme-free reactions were included to be used as background controls. KLK5 was also treated with the same inhibitor concentration and incubation time as a control and for comparison purposes.

In Vitro Identification of Potential KLK8 Substrate Targets

Mat-KLK8 Activation of Pro-KLK1, Pro-KLK11, and Pro-KLK5—Pro-KLK1 and active KLK8 were incubated at a 1:1 molar ratio in a total volume of 50 μl at 37 °C for 10- and 30-min time points. Reactions were done in triplicate. Given the issues of pro-KLK1 autoactivation and similar trypsin-like activity of mat-KLK8, KLK1-specific activity was measured by detecting fluorescence release of pulled down KLK1 before and after incubation with mat-KLK8, as described previously (33).

Pro-KLK11 (1 μM) and active KLK8 (10 nM) were incubated at a 1:100 molar ratio in a total volume of 50 μl at 37 °C for 0.5-, 1.5-, and 3-h time points in optimal KLK8 activity buffer. Detection of activation was done in triplicate where 10 μl of the activation mix was added to 90 μl of KLK11-optimized assay buffer (50 mM Tris, 1.0 M NaCl, 0.01% Tween 20, pH 8.5) containing 0.25 mM PFR-AMC.

KLK5 (20 nM) and active KLK8 (20 nM) were incubated in a total volume of 50 μl at 37 °C for 1- and 3-h time points in optimal KLK8 activity buffer. Detection of activation was tested in triplicate where 10 μl of the activation mix was added to 90 μl of KLK5-optimized assay buffer (100 mM sodium phosphate, 0.01% Tween 20, pH 8.0) containing 0.1 mM FSR-AMC. The increase in fluorescence signal was measured on a Wallac Victor fluorometer, as described above.

Mat-KLK8 Proteolytic Processing of LL-37 Cathelicidin Antimicrobial Peptide—For analysis of LL-37 processing by mat-KLK8, 140 μM LL-37 synthetic peptide was incubated with 20 nM KLK8 for 0, 2, and 6 h at 37 °C in total volume of 400 μl of 50 mM Tris-HCl buffer containing 2 M NaCl, pH 8.50. After incubation, peptides were separated by two independent methods as follows: 1) peptide separation by reverse-phase HPLC (Agilent Eclipse XDB-C18, 5 μm) followed by peptide identification by LC/MS, and 2) direct peptide separation and identification of the LL-37/KLK mixture by LC/MS/MS.

In the first method, the C18 column was equilibrated in 10% acetonitrile with 0.1% trifluoroacetic acid at a flow rate of 0.8 ml/min for 10 min, and cleaved peptides were eluted using a 30-min gradient of 10–100% acetonitrile. Column effluent was monitored at 214 and 280 nm, and one fraction was collected per min. All collected 0.8-ml fractions were lyophilized prior to pre-concentration using the OMIX C18MB (Varian) tips and eluted with 5 μl of buffer A (0.1% formic acid and 0.02% trifluoroacetic acid in 65% acetonitrile). In the second method, the incubation mix was purified and pre-concentrated using the OMIX C18MB (Varian) tips and immediately applied to a mass spectrometer setup with C18 trap column using the EASY-nLC system (Proxeon Biosystems, Odense, Denmark). Recombinant KLK14 ability to process LL-37 was tested given that this possibility was not previously investigated. KLK5 cleavage of LL-37 was included as a positive control.

Effect of Calcium Induction of Terminal Keratinocyte Differentiation on KLK8 Expression

HaCat cells were cultured in low serum EpiLife medium (Invitrogen) containing 0.06 mM calcium. One million HaCat cells were seeded in two T-175 flasks from the same passage (passage 3). In the calcium-treated flasks, HaCat cells in low calcium (0.06 mM) basal condition were switched to high calcium (2.0 mM) at 20% confluency. Calcium-treated and non-treated cells were allowed to reach 70% confluency prior to switching to EpiLife serum-free medium containing no added supplements. One-ml aliquots of the serum-free medium were collected each day for 3 days to measure total protein and KLK8 levels.

Collection and Preparation of Sweat and Stratum Corneum Tissue Extracts

Sweat samples were collected from the face, arms, legs, stomach, and abdomen of seven healthy donors during a dry sauna session. Volunteers showered the night before and had not applied any topical agents to their skin. Sweat samples were collected using 1-ml pipettes into 15-ml tubes and snap-frozen on dry ice prior to storage at −20 °C. On the other hand, stratum corneum flakes were collected from eight volunteers using previously described "tape-stripping" (36) and "scraping" methods (37). The "scraping method" generated a higher number of total protein extracts during method optimization, and hence this procedure was used for the actual study. Briefly, scraping buffer (50 mM sodium phosphate buffer, pH 7.2, containing 5 mM EDTA, 150 mM NaCl, 0.1% Tween 20) was applied to the forearm of each volunteer, and

it was spread evenly to moisten. A microscope slide was then used to scrape the skin surface until corneocyte cells were visible on the slide. The corneocytes were washed off the slide into a 50-ml tube with 10 ml of buffer and soaked for 10 min prior to storage at −20 °C. For processing, sweat and SC samples were thawed, vortexed for 10 min, and centrifuged at 4000 rpm, 4 °C for 15 min. Sweat samples were pooled and dialyzed using a 3-kDa membrane to remove salts. Dialyzed pooled sweat and pooled SC samples were next passed through a Millipore 0.22-μm filter (Nalgene syringe filters, 0.2 μm; 25 mm) and finally concentrated 20× using Amicon ultracentrifugal filters with a 3-kDa molecular mass cutoff. Concentrated and pooled sweat and SC tissue extracts were stored at −20 °C until analysis. Sweat and SC solubilized total protein amounts were quantified using the BCA assay (Pierce).

Immunodetection of KLK8 Expression in Normal Human Sweat, SC, and Skin Cell Culture via a KLK8-specific Enzyme-linked Immunosorbent Assay (KLK8-ELISA)

KLK8 concentration in sweat and SC tissue extracts as well as in the culture media of HaCat keratinocytes, primary human epidermal keratinocytes, epidermal melanocytes, and dermal fibroblasts was determined by a monoclonal-monoclonal KLK8 sandwich-type ELISA. In the case of culture media, primary human epidermal keratinocytes, primary human epidermal melanocytes, and primary human dermal fibroblasts from neonatal human foreskin were purchased from Cascade Biologics (Invitrogen) and cultured according to the manufacturer's instructions. The HaCat keratinocyte cell line was grown in DMEM containing 10% FBS. HaCat cells were plated at a seeding density of 3.0×10^4 cells/well, and primary human epidermal keratinocytes, primary human epidermal melanocytes, and primary human dermal fibroblast cells were seeded at a density of 2.0×10^5 cells/well in 6-well plates. The medium was changed after 48 h, when cells were 60–80% confluent, to a fresh medium (5 ml), and this day was marked as day 0. Aliquots of the medium from each well of the 6-well plates were collected daily for 12 days. Secretion of epidermal KLKs such as KLK5–7, -11, -13, and -14 was also investigated by KLK-specific ELISAs. To control for the viability of cells, the levels of the intracellular enzyme lactate dehydrogenase were measured as an internal control in the culture media to indicate cell membrane rupture and cell death over time.

Immunocapture of KLK8 Activity in Sweat and SC Epidermal Protein Extracts

Physiologically relevant KLK8-specific activity was measured by detecting AMC fluorescence emission increase after adding VPR-AMC substrate to wells containing immunocaptured or pulled down KLK8 compared with background. Briefly, 500 ng of KLK8-specific monoclonal antibody (mono-Ab 19-10) were immobilized overnight on a 96-well plate in coating buffer (50 mmol/liter Tris, 0.05% Tween 20, pH 7.8). The plate was washed three times with washing buffer (50 mmol/liter Tris, 150 mmol/liter NaCl, 0.05% Tween 20, pH 7.8). About 30 μl of sweat (~40 ng of KLK8), 40 μl of SC extracts (~4 ng of KLK8), and 30 μl of recombinant mat-KLK8 (~250 ng), as well as 10× diluted samples in a total volume of 100 μl of 100 mM sodium phosphate buffer, pH 7.5, were loaded per KLK8 antibody-coated well in triplicate. The plate was incubated at room temperature with gentle shaking for 3 h, and then washed six times with the washing buffer, above, to remove contaminants as well as nonbound KLK8. Subsequently, 200 μl of 0.50 mM VPR-AMC substrate in KLK8 activity buffer at optimal pH 8.5 or 5.0 was added to each well. The substrate was incubated with the immunocaptured KLK8 for a total of 24 h at 37 °C. The increase in fluorescence release was measured in real time at 20-min intervals on a Wallac Victor fluorometer, set at 355 nm for excitation and 460 nm for emission. For controls, recombinant active mat-KLK8, mat-KLK5, and lysyl endopeptidase were loaded into wells coated with KLK8 antibody in the same plate. To test if the sweat and SC contain latent pro-KLK8 that can be activated by potential activators, sweat and SC samples were spiked with active KLK5 or lysyl endopeptidase at 1:100 and 1:1000 molar ratios, respectively, overnight at 37 °C prior to loading into wells coated with KLK8 antibody.

RESULTS

Recombinant Mat-KLK8 and Pro-KLK8 Enzyme Production and Characterization

To characterize KLK8 substrate specificity, regulation, and activation, recombinant mature and pro-KLK8 proteins were produced in their native forms, without any fusion tags, in yeast (*P. pastoris*). Mat-KLK8 was secreted in the yeast culture supernatant after 1 day of 1% methanol induction, with the highest levels produced on day 6 for both mat-KLK8 and pro-KLK8. Recombinant mat-KLK8 was obtained with >95% purity, as verified by silver-stained reduced SDS-PAGE (supplemental Fig. 1), and was confirmed to be pure by mass spectrometry. Around 15 mg of mat-KLK8 protein/liter of supernatant was obtained from yeast cells (supplemental Table 2). The yield of purified mat-KLK8 and pro-KLK8 from 1 liter of culture supernatants was in the range of 0.8–1.5 mg, as determined by ELISA and BCA total protein assays.

Prepro-KLK8 is a 260-amino acid protein comprised of a signal sequence (Met^1–Ala^{28}) followed by a short four-amino acid propeptide (Gln^{29}–Glu^{30}–Asp^{31}–Lys^{32}) and a 228-amino acid trypsin-like serine protease domain (Val^{33}–Gly^{260}), with a predicted zymogen activation site at Lys^{32}–Val^{33} and the serine protease catalytic triad (His^{86}, Asp^{120}, and Ser^{212}) (22). The apparent mass of both purified pro-KLK8 and mat-KLK8 recombinant proteins on a reduced SDS-PAGE was higher (~31 kDa) than their predicted molecular mass (~28 kDa) (Fig. 1*A*). Purified recombinant pro-KLK8 and mat-KLK8 proteins had a similar molecular mass as it was not feasible to differentiate molecular mass differences of less than 1 kDa, corresponding to the pro-KLK8 peptide (QEDK), in an SDS-polyacrylamide gel.

KLK8 has one predicted glycosylation site at ^{100}NSS. We detected recombinant KLK8 glycosylation upon treating both mat-KLK8 and pro-KLK8 enzymes with PNGase F (Fig. 1*B*). The nonglycosylated reduced form of KLK8 shifted lower

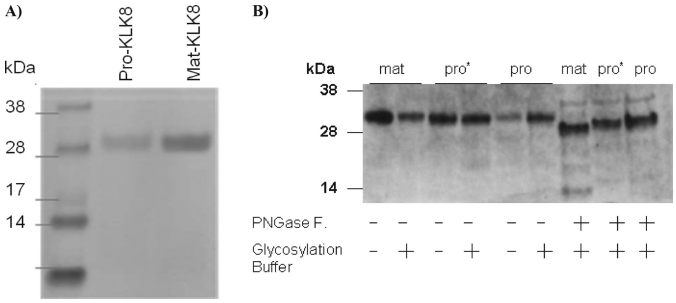

FIGURE 1. **Recombinant pro-KLK8 and mat-KLK8 protein expression and glycosylation.** *A,* Coomassie-stained reduced SDS-PAGE of purified pro-KLK8 (*1st lane*) and mat-KLK8 (*2nd lane*). *B,* Western blotting confirming the identity of the purified mat-KLK8 and pro-KLK8 proteins and their glycosylation. PNGase F treatment of recombinant pro- and mat-KLK8 resulted in deglycosylation (from 31 to 28 kDa) in a reduced SDS-PAGE. Pro-KLK8 *with asterisk* refers to crude pro-KLK8 prior to size exclusion second purification and *without asterisk* refers to pro-KLK8 after final purification.

from an apparent molecular mass of 31 to 28 kDa. Glycosylation of KLK8 was detected under both reduced and nonreduced conditions (supplemental Fig. 2*B*).

Although purified mat-KLK8 appeared as an intact 31-kDa band at the time of purification, we detected three lower bands at 21, 11, and 8 kDa after keeping the enzyme at 4 °C for a week in PBS buffer, pH 7.4 (Fig. 2*A, lanes 1–3*). Western blotting and N-terminal sequence analysis identified the low molecular mass (<28 kDa) bands as internal fragments of mat-KLK8, likely arising from autoproteolytic cleavage (Fig. 2, *B* and *C*). The N-terminal sequence of the top two bands, band I and band II, was determined to be VLGGHE by Edman degradation, which corresponds to the N-terminal sequence of active mature KLK8. The lower two bands were identified as autodegradation products of mat-KLK8 having an internal N-terminal sequence of ENFPDT, indicating autocleavage after Arg^{164} (Fig. 2*C*). By homology modeling using the PyMOL software, we found that Arg^{164} resides in an exposed, solvent-accessible surface loop, which is consistent with being susceptible to autolysis (Fig. 2*D*). The purified pro-KLK8 was visualized as a single glycosylated band of 31 kDa, with an N-terminal sequence of QEDKV as expected.

Recombinant Mat-KLK8 Activity and pH Profiling

To verify the activity recombinant mat-KLK8 activity, gelatin zymography was performed. Interestingly, the top two bands with an N-terminal sequence of VLGGHE were both active in degrading gelatin (Fig. 2*B*). Hence, it is likely that band II resulted from a C-terminal cleavage likely after Arg^{235} or Arg^{247} that did not affect the protease active site (Fig. 2*C*). The lower two bands (bands III and IV) were not active in degrading gelatin, consistent with having an internal N-terminal sequence of ENFPDT, missing active histidine (His^{86}) and aspartic acid (Asp^{120}) residues of mat-KLK8 catalytic triad (Fig. 2*C*).

We also verified the mat-KLK8 ability to cleave fluorogenic AMC substrates and showed that it is able to cleave VPR-AMC substrate efficiently. The pH dependence of the KLK8 activity was checked in several buffer systems, *i.e.* 100 mM sodium acetate (pH 4.5–5.5), PBS (pH 6–7.5), and 50 mM Tris buffer with 2 M NaCl (pH 8–9). The pH range of 7–9 was optimal with pH 8.5 resulting in the highest activity (data not shown). We compared 50 mM Tris-HCl buffer to 100 mM sodium phosphate buffer, at the optimal pH range of 8, 8.5, and 9. KLK8 was most active at pH 8.5 in both buffers, but it displayed 2.5-fold higher activity in the phosphate buffer (data not shown). Furthermore, KLK8 showed 1.25-fold higher activity when 0.01% Tween 20 was added as a carrier in the reaction mix. Therefore, 100 mM phosphate, 0.01% Tween 20 (pH 8.5) was the optimal KLK8 "activity buffer" used for kinetic studies.

KLK8 displayed minimal activity at pH 5.0 initially, but higher activity was detected when the reaction was left overnight at room temperature. These results agreed with our detection of autodegradation products of mat-KLK8 after 1 week of incubation at 4 °C in PBS buffer (pH 7.4), suggesting the ability of KLK8 to cleave itself at pH 7.4 even at a low temperature of 4 °C.

Regulatory Modes of KLK8 Activity

Mat-KLK8 Autodegradation Leads to in Vitro Enzymatic Inactivation—To investigate a potential KLK8 autodegradation process, we performed a stability time course study. Autodegradation fragments were detected after 12 h of incubation at 37 °C on a reduced silver-stained SDS-PAGE (Fig. 2*E*). Mat-KLK8 activity increased initially upon incubation at 37 °C and decreased only when autodegradation bands were detected 12, 24, and 34 h later. After 24 and 34 h of incubation at 37 °C, the intact mat-KLK8 band at 31 kDa disappeared, and cleaved fragments represented the majority of KLK8 present. This correlated with a reduction in residual activity to 18 and 9% after 24 and 34 h incubations, respectively (Fig. 2, *E* and *F*). No autodegradation products or significant changes in mat-KLK8 activity were detected in the enzyme samples incubated at 4 and 25 °C at the same time points up to 24 h (data not shown). To ensure that mat-KLK8 degradation after Arg^{164} was not due to contaminating host proteases, the purity of recombinant mat-KLK8 was analyzed by mass spectrometry where only KLK8 and a small amount of keratin were identified.

Mat-KLK8 was also incubated alone and in the presence of protease inhibitors of different classes. As shown in Fig. 2*G*, mixture inhibitors and general serine protease inhibitors such as PMSF completely abolished KLK8 activity. The inhibitor AT has no effect on KLK8 activity, although it is an efficient inhibitor of many trypsin-like serine proteases, including trypsin, KLK5, and KLK14. Hence, the same decrease in activity occurred after incubating mat-KLK8 alone or in the presence of AT inhibitor for 12 h at 37 °C (Fig. 2*G*). Thus, our data suggest that KLK8 undergoes degradation after Arg^{164} leading to enzymatic inactivation and that this degradation process is likely due to KLK8 activity as it is not prevented by α_1-antitrypsin. To avoid KLK8 autodegradation during enzymatic assay, we determined that mat-KLK8 is stable up to 12 months if stored in aliquots in its elution buffer (0.01 M acetic acid containing 250 mM NaCl, pH 4.76) at −80 °C and for a month if stored similarly at −20 °C.

Glycosylation Effect on Mat-KLK8 Activity—It is highly unlikely that the *N*-glycan attached to Asn^{100} of KLK8 participates in its substrate binding as it is directed away from the catalytic triad and substrate binding pocket (Fig. 2*D*). Our results confirmed that deglycosylation had no effect on the ability of mat-KLK8 to cleave VPR-AMC (supplemental Fig. 2).

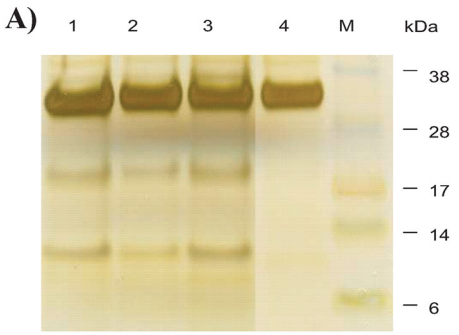

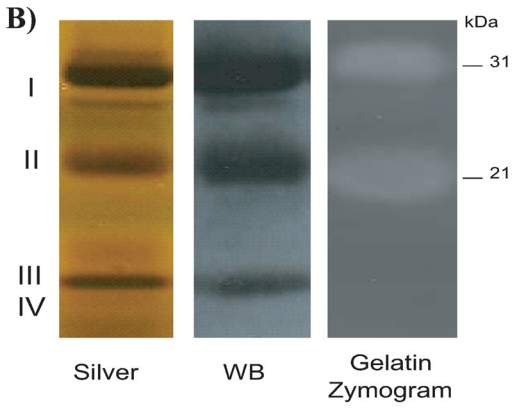

C)

1 MGRPRPRAAK TWMFLLLLGG AWAGHSRA^{28} QE DK^{32} VLGGH ECQ PHSQPWQAAL FQGQQLLCGG

61 VLVGGNWVLT AAHCKKPKYT VRLGD(H^{86})* SLQN KDGPEQEIPV VQSIPHPCY N^{110} SSDVEDHNH (D^{120})*

121 LMLLQLRDQA SLGSKVKPIS LADHCTQPGQ KCTVSGWGTV TSPR^{164} ENFPDT LNCAEVKIFP

181 QKKCEDAYPG QITDGMVCAG SSKGA D^{206} TCQG D (S^{212})* GGPLVCDG ALQGITSWGS DPCGRSDKPG

241 VYTNICRYLD WIKKIIGSKG

I, II

III, IV

D)

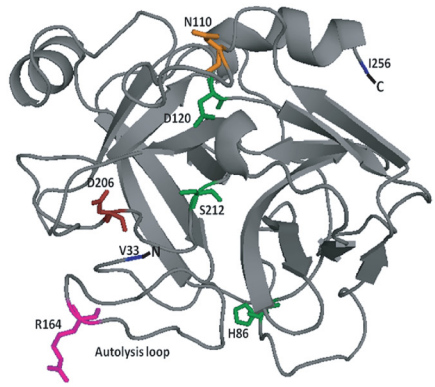

E)

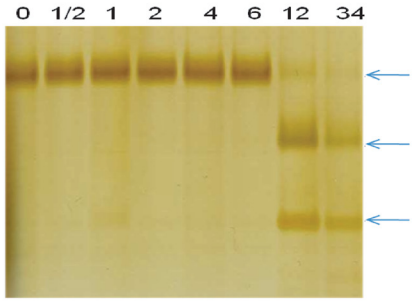

F)

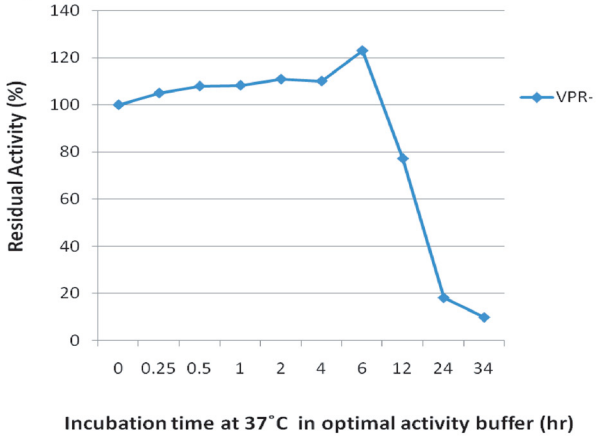

G)

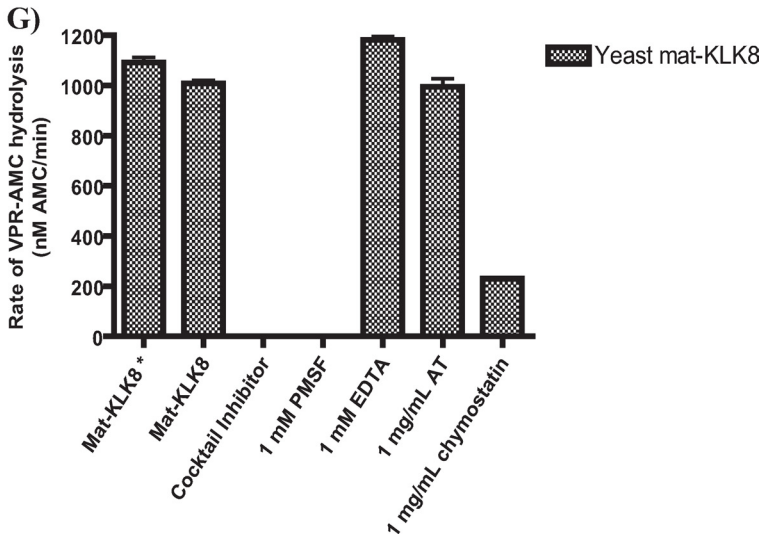

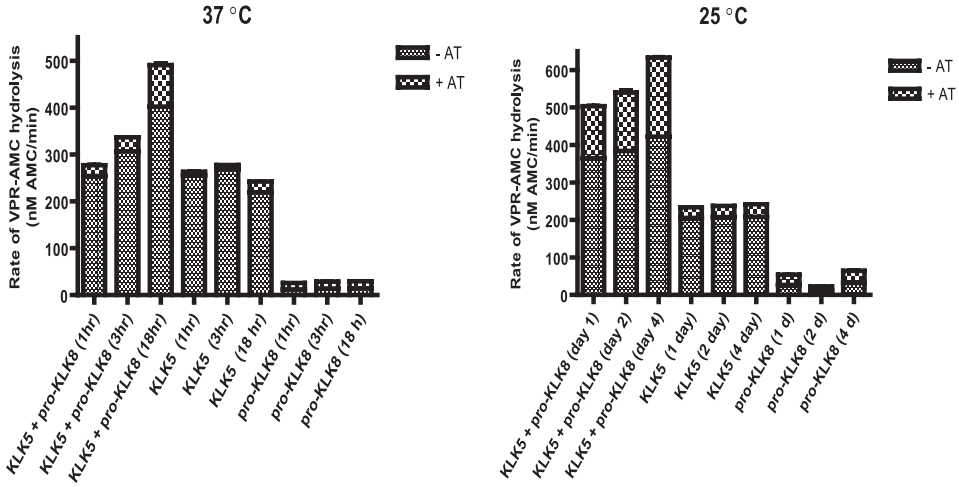

FIGURE 3. **Pro-KLK8 activation by active KLK5.** Activation or pro-KLK8 by mat-KLK5 was carried at a molar ratio of (10:1), where a duplicate mix was included with AT as a KLK5 activity quencher. Each activation mix was incubated for varying time points (1, 3, and 18 h at 37 °C or 1, 2, and 4 days at 25 °C) with or without an additional 1-h incubation with AT. Activity toward VPR-AMC substrate was measured for the same reaction mixtures with or without AT in triplicate.

Pro-KLK8 Zymogen Activation—Pro-KLK8 is activated by trypsin-like cleavage at Lys^{32}–Val^{33}. Stratum corneum trypsin-like enzyme or KLK5 is thought to be the "initiator" a pro-KLK activation cascade in human epidermis because of its autoactivation in human SC. Hence, we aimed to test the ability of KLK5 to activate pro-KLK8 *in vitro*. One of the obstacles in identifying endogenous activators of pro-KLKs is the lack of specific activity assays that differentiate between the trypsin-like activity of the potential activator and the pro-KLK under investigation. To avoid confounding activity results because of overlapping KLK5 and KLK8 trypsin-like activity, AT inhibitor was used in this study to quench KLK5 activity prior to detecting pro-KLK8 activation. As a control, we showed that AT decreased mat-KLK5 activity to less that 3% of its original activity, and it had no inhibitory effect on mat-KLK8 activity at all (Fig. 3). The significant increase in activity detected in the pro-KLK8/mat-KLK5 mix after 1 day of incubation at 25 °C and 18 h at 37 °C, after quenching KLK5 activity with AT, indicated activation of pro-KLK8 (Fig. 3). Although KLK5 is indeed an *in vitro* activator of pro-KLK8, this activation process was slow as it occurred after 18 h of incubation at 37 °C. Nonetheless, KLK5 activation of pro-KLK8 may be important physiologically as normal human epidermal cell turnover occurs in the span of 2–4 weeks. Furthermore, expression data suggest that immunoreactive KLK8 concentration in normal human SC tissue extracts is about 4-fold higher than KLK5 (21). Hence, this activation process may occur quicker had we used a pro-KLK8:KLK5 molar ratio of 1:4 or 1:1 instead of 1:10.

We next tested if KLK8 is activated by KLK1 given that KLK1 is active in normal human sweat (38) and co-localizes with pro-KLK8 in the SC. We used a pro-KLK1 preparation known to autoactivate and found that the KLK8 was not activated by KLK1 activity even after 48 h at 37 °C and 4 days of incubation at 25 °C (data not shown). Autoactivation of pro-KLK8 was not reported previously; however, we detected a time- and concentration-dependent increase in AMC fluorescence emission after incubating pro-KLK8 for 48 h at 37 °C and 4 days at room temperature (supplemental Fig. 3*B*). This very slow autoactivation was questionable as it could have been facilitated by host proteases. We thus carried out a stability time course study using two recombinant pro-KLK8 enzymes produced in baculovirus and yeast expression systems. Pro-KLK8 proteases were incubated in the presence of

FIGURE 2. **Activity and autodegradation of recombinant mat-KLK8.** *A,* silver-stained reduced SDS-PAGE of purified mat-KLK8 (*lanes 1–4*). *Lane 4* represents intact purified recombinant mat-KLK8 protein at 31 kDa. *Lanes 1–3* represent the purified mat-KLK8 protease after storage in PBS buffer, pH 7.4, at 4 °C for 7 days. *B,* detection of active mat-KLK8 and degraded fragments in replicate silver-stained SDS-PAGE, Western blotting, and gelatin zymography. Intact KLK8 corresponded to the 31-kDa band. Lower molecular weight autodegradation fragments of KLK8 are labeled *II–IV* having an apparent molecular mass of 21, 11, and 8 kDa. Only bands I and II were active as revealed by the two *white bands* in the gelatin zymogram. *C,* location of the N-terminal sequences obtained by Edman degradation of each KLK8 autodegradation fragment within the primary KLK8 protein sequence. Prepro-KLK8 is formed of a signal peptide, followed by a short 4-amino acid propeptide (*boldface* and *underlined*) and the mature KLK8 N-terminal sequence (*boldface* and *boxed*). The N-terminal sequence of KLK8 degradation fragments *II–IV* is *boxed*, with the corresponding label *above*. The Arg^{164} amino acid where autolytic cleavage occurs is *boldface*. The catalytic triad (His^{86}, Asp^{120}, and Ser^{212}) is indicated with an *asterisk*. The site of putative processing by a signal peptidase is C-terminal to Ala^{28}, and Lys^{32} marks the activation site of the pro-KLK8 protease, the Asn^{110} glycosylation site, and Asp^{206}, which confers trypsin-like specificity of the mat-KLK8 protease, are *boldface,* and *labeled* with their position in the KLK8 primary sequence. KLK8 sequence is numbered from the N terminus of prepro-KLK8 based on NCBI GenBank™ accession number NP_009127. *D,* location of key residues and the autolytic cleavage site within the theoretical tertiary structure of mature KLK8, as predicted by PyMOL homology modeling. The ribbon plot of mature KLK8 is shown in the traditional serine protease standard orientation (*i.e.* looking into the active site cleft). Secondary structure elements are displayed as *arrows* (β-strands) and *ribbons* (α-helices). N- and C-terminal residues are shown in *black*. The side chains of the catalytic triad residues are shown in *green*. Asp^{206} is shown in *red* at the base of the active site pocket. The glycosylation site is colored *orange*. KLK8 autocleavage site after Arg^{164} at P1 is shown in *magenta*. *E,* silver-stained SDS-PAGE displaying mat-KLK8 autodegradation in a time course study. Cleaved fragments represented the majority of KLK8 detected after 12-h incubations at 37 °C. *F,* mat-KLK8 autolysis resulted in enzymatic inactivation detected by the drastic decrease in residual KLK8 activity toward VPR-AMC at time points 12, 24, and 34 h, corresponding to residual activity of 78, 18, and 9%, respectively. *G,* mat-KLK8 activity in the presence of inhibitors of different protease classes. The mat-KLK8 labeled with an *asterisk* was not incubated at 37 °C, although the remaining samples were incubated for 12 h at 37 °C.

TABLE 1
Divalent ion effect on mat-KLK8 activity

Ion[a]	Concentration[b]	Molar ratio	Residual activity
	mM	*KLK8:cation*	*(100%)*
Ca^{2+}	0.0001	(1:10)	114.9
	0.001	(1:100)	116.5
	0.10	(1:10,000)	121.0
	1.00	(1:100,000)	145.0
	10.0	(1:1,000,000)	150.2
Mg^{2+}	0.10	(1:10,000)	106.1
	1.00	(1:100,000)	112.8
	10.0	(1:1,000,000)	142.0
Zn^{2+}	0.0001	(1:10)	105.4
	0.001	(1:1,00)	101.2
	0.01	(1:1,000)	107.3
	0.10	(1:10,000)	76.6
	1.00	(1:100,000)	39.6
	10.0	(1:1,000,000)	28.6
Na^{+}	10.0	(1:1,000,000)	100
K^{+}	10.0	(1:1,000,000)	100

[a] Ca^{2+} and Na^{+} data correspond to incubation of KLK8 with $CaCl_2$ or NaCl, respectively.
[b] KLK8 final concentration was 0.00001 mM (or 10 nM) in all experiments.

inhibitors of different protease classes, similar to the experiment performed previously to investigate mat-KLK8 autodegradation (Fig. 2*G*). We detected an increase in AMC fluorescence emission upon incubating both proteases alone at 37 °C for 48 h. However, unlike mat-KLK8 autodegradation, pro-KLK8 activation was facilitated by host serine proteases that were inhibited by AT treatment (supplemental Fig. 3*B*). For *in vitro* activation of pro-KLK8, lysyl endopeptidase was the best pro-KLK8 activator, due to its specific cleavage after lysine residues, where it resulted in rapid activation of pro-KLK8 (16.5-fold increase) within 1 h of incubation at 37 °C with 1:1000 (activator:pro-KLK8) ratio (data not shown). Thus, our data show that pro-KK8 does not autoactivate or get activated by KLK1, but it is activated by KLK5 and lysyl endopeptidase *in vitro*.

Effect of Cations—The ability of the KLK8 activity to hydrolyze VPR-AMC in the presence of the relevant epidermal cations Zn^{2+}, Ca^{2+}, Mg^{2+}, Na^{+}, and K^{+} was examined, as shown in Table 1. KLK8 was activated to a significant extent by Ca^{2+} ions at all concentrations examined. Mg^{2+} ions activated KLK8 but to a lower extent compared with Ca^{2+} and at higher concentrations. On the other hand, Zn^{2+} attenuated mat-KLK8 activity as expected given its inhibitory effect on numerous metal-binding enzymes, including metalloproteases and other KLKs. Zn^{2+} inhibition of 10 nM mat-KLK8 was pronounced in the micromolar and millimolar range but not in the nanomolar range. Na^{+} and K^{+} cations had no significant effect on KLK8 activity at the concentrations tested. These results supported the involvement of metal ions, particularly Ca^{2+} and Zn^{2+}, at the active site of mat-KLK8. To date, the crystal structure of human KLK8 remains to be resolved; thus, the exact mechanisms by which zinc and calcium bind the human KLK8 active site remain to be elucidated.

Inhibition by Skin-specific Inhibitors and General Serpins—We investigated the inhibitory effects of three serine protease inhibitors known to be present in human SC as follows: the lymphoepithelial azal type inhibitor (LEKTI), SLPI, and elafin. SLPI and elafin did not inhibit mat-KLK8 activity (data not shown). These inhibitors inhibit chymotrypsin-like KLK7 activity but do not exert any inhibitory effect on other epidermal trypsin-like KLKs (39). Alternatively, inhibitory LEKTI domains (D1–15) inhibit distinct trypsin-like KLKs and chymotrypsin-like KLK7 with different potencies (40, 41). LEKTI inhibition of epidermal serine proteases is abolished in the skin disease Netherton syndrome characterized by *SPINK5* mutations leading to LEKTI truncation and dysfunction. Unlike other epidermal KLKs such as KLK5, KLK6, KLK7, KLK13, and KLK14, and similar only to KLK1 (39), all LEKTI domains had no inhibitory effect on mat-KLK8 activity, even at a 10-fold higher molarity (data not shown). All LEKTI domains tested inhibited KLK5 as a positive control.

We further tested mat-KLK8 inhibition by general serine protease inhibitors (serpins). We confirmed KLK8 inhibition by α_2-antiplasmin, protein C inhibitor, and aprotinin. Unlike KLK5 and KLK14, mat-KLK8 was inhibited by the chymotrypsin-like inhibitor chymostatin but was not inhibited by the trypsin-like inhibitor α_1-antitrypsin (data not shown). Taken together, our results suggest that KLK8 regulation by endogenous inhibitors and general serpins is different from other trypsin-like KLKs such as KLK5 and KLK14.

KLK8 Substrate Specificity

AMC Substrate Profiling and Steady-state Kinetic Constants—The substrate specificity of KLK8 was assessed by profiling its kinetic parameters (*i.e.* K_m and k_{cat}) against a panel of 16 tripeptide synthetic substrates containing an AMC fluorogenic leaving group. Among these AMC peptides, 13 were candidate trypsin-like enzyme substrates (10 with Arg and 3 with Lys basic residues at the P1 position according to the Schechter and Berger notation), and 2 for chymotrypsin-like enzymes (with bulky, hydrophobic amino acids Tyr and Phe), and 1 substrate for neutrophil elastase (with small aliphatic Val at the P1 position). As predicted by the presence of Asp^{206}, close to Ser^{212} of the catalytic triad, KLK8 was confirmed to have trypsin-like but not chymotrypsin-like activity, because no reaction was observed for the two chymotrypsin-like enzyme substrates (AAPF-AMC and LLVY-AMC). The results are presented in Table 2. Mat-KLK8 displayed trypsin-like specificity with a greater catalytic efficiency for Arg *versus* Lys at the P1 position, as substrates with the highest k_{cat}/K_m values contained P1-Arg. Although KLK8 did not cleave GPK, it cleaved VLK, indicating that is it capable of cleaving after lysine, depending on adjacent residues. The P2 specificity of KLK8 was examined by comparing the k_{cat}/K_m values among substrates with invariable P1 and P3 residues as follows: 1) QAR-AMC, QGR-AMC, and QRR-AMC; 2) LKR-AMC and LRR-AMC; and 3) GPR-AMC and GRR-AMC. As shown in Table 1, KLK8 preferred Ala > Arg > Gly, Arg > Lys, and Gly > Pro at P2. This suggested that the P2 position may not influence mat-KLK8 specificity significantly, but this observation was based on comparing a small number of fluorogenic tripeptides. The P3 preference of KLK8 was assessed by examining k_{cat}/K_m values in substrates bearing the same P1 and P2 amino acids as follows: 1) VPR-AMC and GPR-AMC; 2) QGR-AMC, and GGR-AMC; and 3) QRR-AMC and LRR-AMC. Glycine was a highly unfavored residue at this position. The best substrates for mat-KLK8 were VPR-AMC, also a

TABLE 2

Steady-state kinetic parameters for the hydrolysis of synthetic AMC substrates by mat-KLK8 in optimal activity buffer (100 mM Na_2HPO_4, pH 8.5)

Boc is *t*-butoxycarbonyl, Tos is tosyl.

Substrate	V_{max} [a]	K_m	k_{cat}	k_{cat}/K_m	Normalized activity [b]
	μmol/min/mg	*mM*	min^{-1}	$mM^{-1}\ min^{-1}$	%
Trypsin-like					
Boc-VPR-AMC	13.08	0.0238 ± 0.025	405.38	17004.31	100
Boc-QAR-AMC	11.14	0.1844 ± 0.009	345.24	1872.253	11
H-PFR-AMC	8.610	0.1533 ± 0.017	266.89	1740.994	10
Boc-QRR-AMC	6.566	0.2247 ± 0.017	203.53	905.7995	5.0
Boc-LRR-AMC	3.136	0.1165 ± 0.004	97.216	834.4745	4.9
Boc-FSR-AMC	6.903	0.2983 ± 0.071	213.98	717.3365	4.2
Boc-LKR-AMC	3.028	0.1407 ± 0.017	93.881	667.2431	3.9
Boc-VLK-AMC	7.039	0.3326 ± 0.023	218.21	656.0810	3.8
Boc-QGR-AMC	2.766	0.3699 ± 0.018	85.751	231.8222	1.4
Benzlyoxycarbonyl-GGR-AMC	2.881	0.4312 ± 0.060	89.307	207.1133	1.2
Tos-GPR-AMC	4.076	0.6897 ± 0.125	126.36	183.2210	1.0
Tos-GPK-AMC	NR[c]	NR			
Boc-EKK-AMC	NR	NR			
Chymotrypsin-like					
AAPF-AMC	NR	NR			
LLVY-AMC	NR	NR			
Negative control					
AAPV-AMC	NR	NR			

[a] For specific activity, V_{max} (μmol/min/mg) = (adjusted V_{max} (FU/min) × calibration factor (μmol of AMC/FU)) ÷ amount of enzyme added (mg).
[b] For normalized activity, k_{cat}/K_m (substrate) ÷ k_{cat}/K_m (Boc-VPR-AMC) × 100%.
[c] NR indicates no reaction.

substrate for α-thrombin, and QAR-AMC, also a substrate for trypsin.

Rapid Endopeptidase Library (RepLi) Screening of Mat-KLK8 P2-P2′ Substrate Specificity—A rapid endopeptidase profiling library of quenched FRET peptides was utilized to reveal information about nonprime and prime side substrate specificity of mat-KLK8. The principle of this assay and how it differed from nonprime AMC substrate profiling is illustrated in Fig. 4. Our data suggest that mat-KLK8 is a specific trypsin-like enzyme, where all top 29 peptide pools displaying strong and moderate cleavage contained Arg/Lys (Fig. 4*B*). Of the 57 peptide pools cleaved, 47 contained Arg/Lys in at least one variable core region, consistent with the trypsin-like specificity of KLK8 on the C-terminal side of basic residues. Interestingly, 10 of the peptide pools that showed weak cleavage (S:B = 1.25–1.50) contained no Arg/Lys, where 9 pools contained Phe/Tyr, and one peptide pool contained Ile/Leu, suggesting restricted weak chymotrypsin-like activity of mat-KLK8. Our data indicate that mat-KLK8 enzyme is likely to function as a regulatory trypsin-like protease in upper epidermis rather than a degrading enzyme with broad specificity, as 122 out of the total 169 peptide pools containing at least one Arg/Lys (~72% of trypsin-like peptides) remained uncleaved after 1 h of incubation (S:B <1.25). KLK8 selectivity can be seen by its *in vitro* ability to activate the pro-form of merpin-β, but not merpin-α, even though activation of both epidermal metalloproteases requires cleavage after arginine (42). The top peptide hit for KLK8 with highest fluorescence increase contained the core motif (RK)(S/T)(A/V) and 6 out of the top 14 peptide hits contained the (R/K)–(S/T) bond, indicating a strong preference for Ser/Thr at P1′ (supplemental Table 3). Using this peptide as a reference for position-scanning profiling of mat-KLK8 specificity, we found that mat-KLK8 displayed a strong preference for hydrophobic Ile/Leu and Phe/Tyr amino acids at P2, specific preference for Arg/Lys at P1, restricted preference for Ser/Thr and Phe/Tyr at P1′, and Ala/Val, Arg/Lys, and Phe/Tyr at P2′ (Fig. 4*C*). All peptides containing negatively charged amino acids (Asp or Glu) at P′1 or P′2 in this library were not hydrolyzed by mat-KLK8. Furthermore, we detected potential subsite cooperativity in the active site pocket, where the presence of two (Arg/Lys) residues close to each other enhanced cleavage (supplemental Table 3). These results were consistent with the unpublished data[3] regarding mat-KLK8 nonprime substrate specificity where KLK8 was found to prefer Arg over Lys at P1, hydrophobic residues at P2, and Arg/Lys residues at P3 (42). Here, we confirmed that cleavage of this 8-peptide pool occurred after arginine by mass spectrometry MS1 (Fig. 4*D*) and identified the fluorescent tag as well as the cleaved N-terminal side of the peptide by MS2 analysis as shown in Fig. 4*E*.

Identification of Potential Substrates by Mat-KLK8

Activation of Co-localized Epidermal Pro-KLKs (Pro-KLK5, Pro-KLK1, and Pro-KLK11)—Pro-KLK5, pro-KLC1, and pro-KLK1 are potential downstream targets of mat-KLK8 given their co-localization with KLK8 in normal human sweat and SC and the requirement for cleavage after Arg for their activation. Pro-KLK10 is an unlikely substrate of mat-KLK8 because its activation sequence NDTRLDP contains two acidic Asp residues, P3-Asp and P2′-D, which are highly unfavored residues for mat-KLK8 based on our RepLi screening. Unfortunately, we were unable to draw any conclusions regarding KLK5 activation by KLK8, because of the confounding effect of KLK5 rapid autoactivation. In the case of pro-KLK1, which autoactivates, we utilized a sandwich-type pulldown assay to capture KLK1 and completely eliminate mat-KLK8 activity. Although KLK8 exhibits activity toward PFR-AMC, no enzymatic activity was observed for the pulled down KLK8 on KLK1 antibody-

[3] M. Debela, E. L. Schinder, and C. S. Craik, unpublished data.

coated wells (Fig. 5*A*). The ability of KLK8 to activate KLK1 was detected in a time-dependent manner (Fig. 5*A*). In the case of pro-KLC1, time-dependent pro-KLK8 activation was seen within a 30-min incubation period at 37 °C at 1:100 (KLK8:pro-KLK11) molar ratio (Fig. 5*B*). Hence, we demonstrated the ability of KLK8 to target the *in vitro* activation of two potential substrates, pro-KLK11 and pro-KLK1, in human SC and sweat.

Mat-KLK8 Processing of LL-37 Antimicrobial Peptide (AP)—Cathelicidin APs are effector molecules of the innate immune system detected in human SC, sweat, and wound secretions

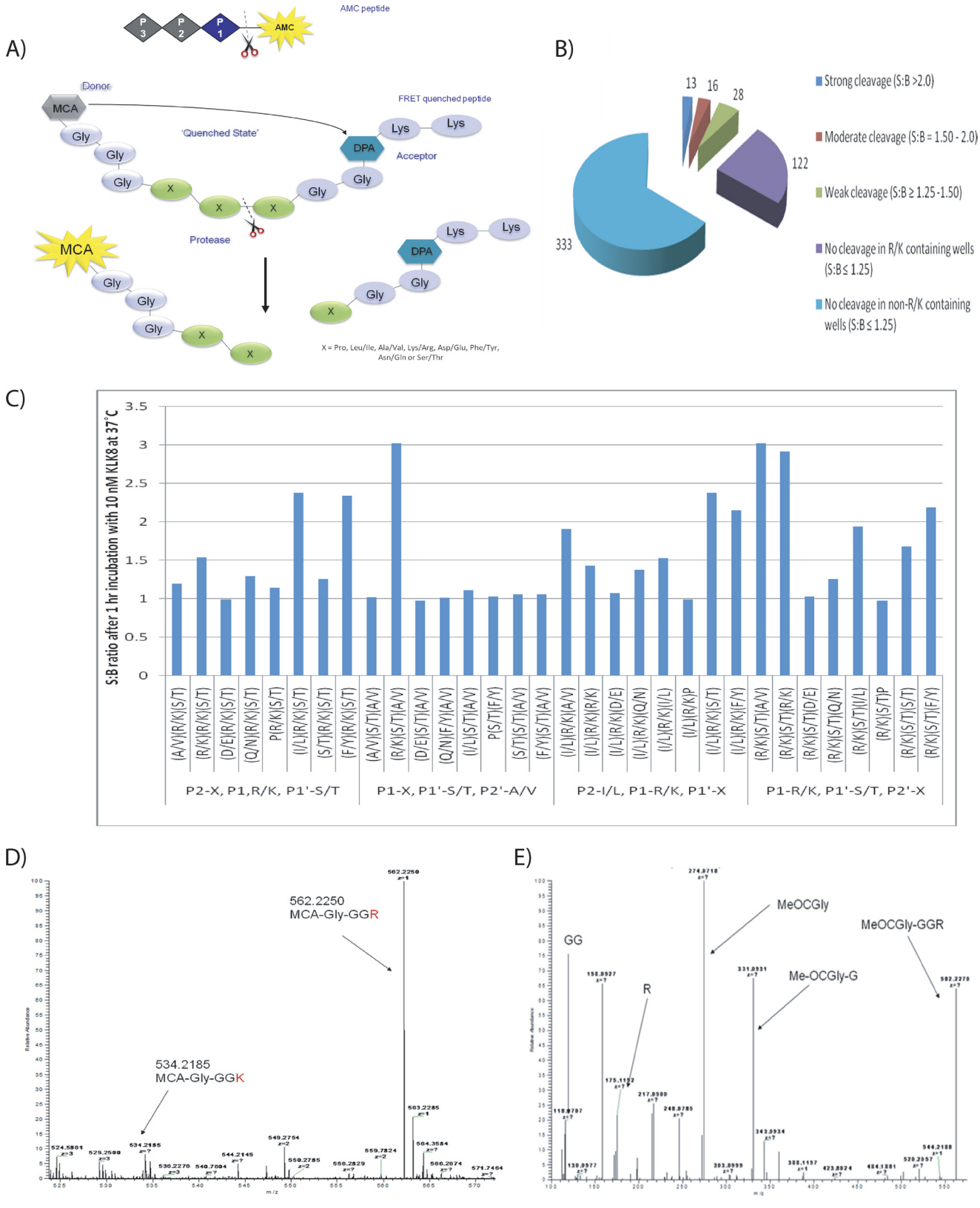

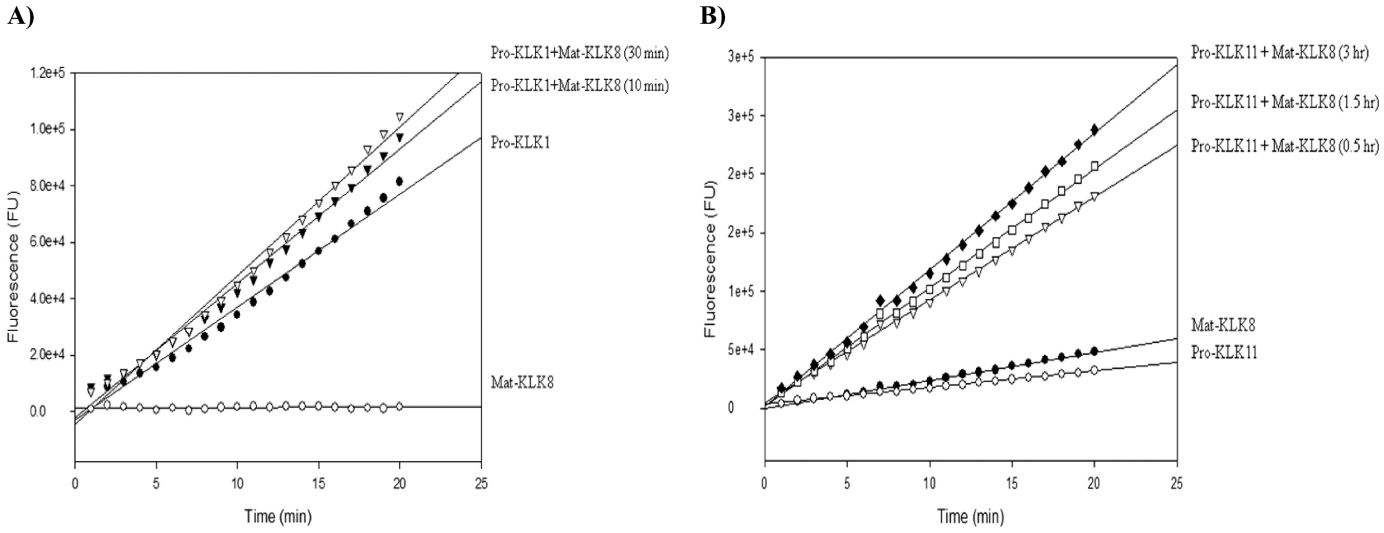

FIGURE 5. **Mat-KLK8 targeting of pro-KLK1 and pro-KLK11 activation.** *A,* pro-KLK1 activation by mat-KLK8 was performed using a sandwich-type pull-down activity assay of pro-KLK1. The activated KLK1 was pulled down using a specific antibody. Mat-KLK8 activity was removed through washes, and KLK1 activation by KLK8 was measured by monitoring the fluorescence release of AMC substrate normalized to the background signal. Enzymatic activity of pulled down KLK1 was measured, using 0.25 mM PFR-AMC. *B,* pro-KLK11 activation by mat-KLK8. Time-dependent activation of pro-KLK11 was detected at a 1:100 molar ratio at 37 °C in optimal KLK8 activity buffer. Pro-KLK11 activation is measured by detecting fluorescence release off 0.25 mM PFR-AMC over time for the pro-KLK11 alone, mat-KLK8 alone, and the pro-KLK11/mat-KLK8 activation mixture as shown above.

with microbicidal and proinflammatory activities (43–45). The 37-amino acid-long C terminus of cathelicidin is referred to as LL-37 and represents the active peptide, which displays direct antimicrobial activity by interaction with the cell membranes of microorganisms. We investigated the ability of KLK8 to process LL-37 synthetic peptide into shorter active antimicrobial peptides. We detected a single peak by RP-HPLC on a C18 column eluting at 55% B, acetonitrile, corresponding to the LL-37 peptide alone which remained present after 2 and 6 h of incubations at 37 °C (supplemental Fig. 4*A*). Processing of the LL37 peptide was observed upon incubation with 20 nM mat-KLK8, where the LL-37 peak seen at 25 min decreased and broadened, and two earlier sharp peaks were detected indicating cleavage of LL-37 (supplemental Fig. 4*B*). The two peaks corresponded to small peptides (charge state $z = 2$) with m/z ratios of 434.2390 and 458.2481, which were identified by LC/MS to represent the LL-7 and NL-8 peptides, respectively. However, the abundance of the remaining cleavage products in the lyophilized RP-HPLC fractions was insufficient to detect by LC/MS. Thus, we used an alternative method where the LL-37 control peptide and LL-37/KLK incubation mixtures were purified by C18 OMIX tips prior to separating on nano-LC C18 column attached directly to LTQ/Orbitrap mass spectrometer. This sensitive method allowed us to identify all peptide fragments present in each sample. We identified the LL-7 and NL-8 fragments as well as IK14, LL-23, and LL-37 in the KLK8-treated sample. LL-37 peptide was treated with active KLK5 as a positive control, and LL-7, NL-8, and IK-6 were identified as cleavage products, in addition to their other halves, KS-30*, LL-29*, KS-22*, which represent the active antimicrobial peptides marked with asterisks, respectively (13). Our results show that active KLK8 and KLK14 process LL-37 AP after Arg residues generating KS-30*/LL-7, LL-29*/NL-8, and IK-14/LL-23* peptides. Fig. 6 displays identified fragments in each LL-37/KLK incubation mix *versus* LL-37 peptide incubated alone for 6 h. IK-14/LL-23* was not identified in the KLK5-treated sample because the IK-14 peptide was likely further proteolyzed to IK-6 and NL-8.

Human KLK8 Is a Keratinocyte-specific Protease Induced during Terminal Keratinocyte Differentiation

To support KLK8 involvement in normal skin barrier functions, we investigated KLK8 secretion by skin cells in culture. Given that KLKs are constitutively expressed in the granular

FIGURE 4. **Mat-KLK8 substrate specificity based on screening rapid endoprotease library of FRET-quenched peptides.** *A,* principle of the REPLi screening of quenched FRET peptides. The peptide library was constructed around a central tri-variable peptide (*XXX*) flanked by Gly residues that link the FRET pair. The diphenylamine (*DPA*) acceptor quenches the 4-methylcoumaryl-7-amide (*MCA*) donor, where excitation at 320 nm produces only a background emission at 420 nm. Upon proteolytic cleavage, the acceptor and donor moieties move apart allowing the 4-methylcoumaryl-7-amide to emit light. Each well contains eight peptide pools with the same variable core region. Potentially problematic amino acids that were removed from the library include Cys (potential for forming disulfide bonds), His (not generally observed within substrates at sites of protease cleavage), Met (because of its hydrophobic and bulky nature being shared by Leu and Ile and its propensity to being oxidized), and Trp (interference with fluorescence signal because of absorbance at $\lambda_{280\ nm}$/emission at $\lambda_{320\ nm}$). Gly was also omitted because cleavage around flanking Gly residues would be detected as background. The remaining 15 amino acids were grouped in matching pairs (Ala/Val, Arg/Lys, Asp/Glu, Asn/Gln, Leu/Ile, Ser/Thr, Phe/Tyr), whereas Pro was left as a single residue to allow access to any potential conformational information. For example, if the variable region in a well contains (R/K)(I/L)(S/T), then the eight tripeptides present there are RIS, RIT, RLS, RLT, KIS, KIT, KLS, and KLT. Compared with the FRET-quenched peptides, the linear AMC-bearing tripeptides shown on the *top* have the dye occupying the P1′-position, and fluorescence occurs only when the covalent bond between P1-AMC is digested by the protease of interest. *B, pie chart* of mat-KLK8 cleavage of RepLi peptides after 1-h incubations with 10 nM mat-KLK8 at 37 °C. *C,* mat-KLK8 specificity based on positional scanning of the top peptide hit result from RepLi screening. *D,* confirmation of top peptide cleavage after arginine by MS1; *E,* identification of the cleaved fragment as well as the MeOGly fluorescent tag by MS2.

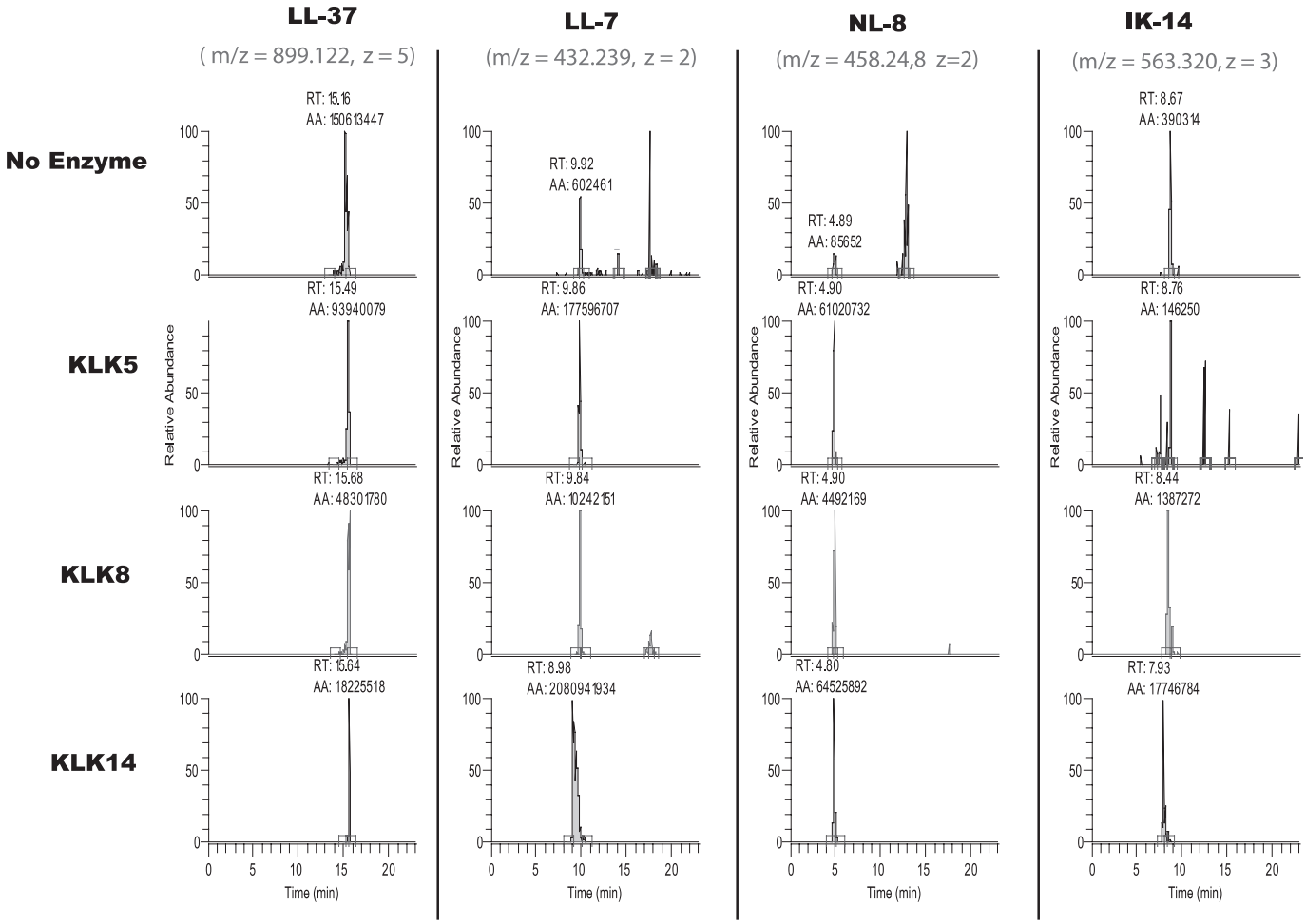

FIGURE 6. **Proteolytic processing of the LL-37 antimicrobial peptide by kallikreins.** Identification of cleaved fragments off LL-37 peptide after 6 h of incubation at 37 °C alone or with active KLK5, KLK8, or KLK14. The MS1 elution profile with integrated peaks is shown for the parent LL-37 peptide, and the LL-7, NL-8, and IK-14 cleaved fragments (labeled at the *top* of the figure with their corresponding *m/z* ratio and *z* charge state) for each of the LL-37 peptides incubated with no enzyme, KLK5, KLK8, and KLK14 as indicated on the *left side* of the figure. The retention times (*RT*) and integrated area under curve (*AA*) are displayed as well. Each of these peptides was confirmed by MS2 in the enzyme-treated samples (data not shown).

layer of epidermis, we cultured HaCat keratinocytes in low *versus* high calcium medium, a manipulation thought to mimic the calcium gradient of upper epidermis (46). We found that increasing exogenous Ca^{2+} in the medium changed keratinocyte cell morphology, induced corneocyte formation as expected (47, 48), and significantly increased KLK8 protein secretion into the medium in a time-dependent manner. We detected over 14-fold increase in KLK8 protein levels in high *versus* low calcium serum-free medium at day 3 (Fig. 7). We also investigated the ability of primary epidermal keratinocytes to co-secrete KLK proteins, including KLK8, as well as other skin cell types such as melanocytes and fibroblasts (supplemental Fig. 5*A*). We found that KLK8 was exclusively secreted by keratinocytes, whereby primary human epidermal melanocyte and primary human dermal fibroblasts secreted no detectable KLK8 even after day 12 in culture. KLK8 levels in the HaCat immortalized keratinocyte and primary neonatal keratinocyte culture media continued to increase with increased keratinocyte proliferation, although lactate dehydrogenase levels remained constant. This confirmed that the elevation in KLK8 levels was due to increased

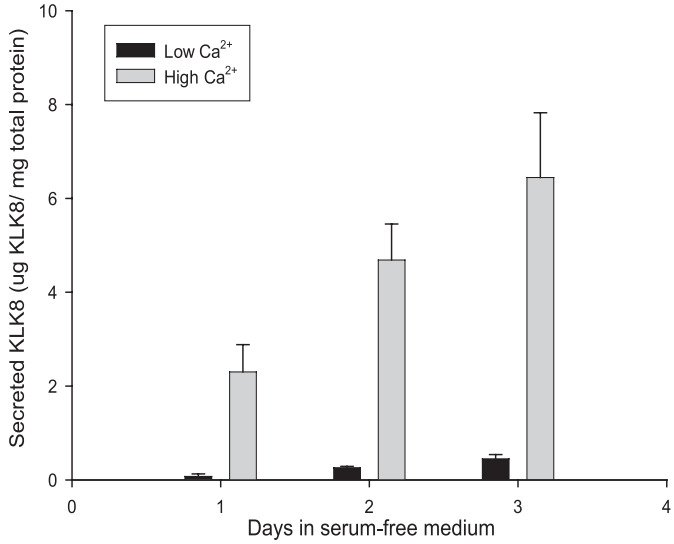

FIGURE 7. **KLK8 protein expression is induced by exogenous calcium ion increase during terminal keratinocyte differentiation.**

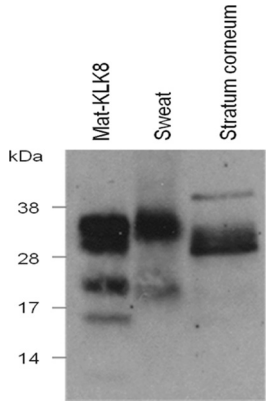

FIGURE 8. **KLK8 is expressed in a free noncomplexed form in normal human sweat and non-palmoplantar stratum corneum.**

secretion rather that cell rupture or death over time (supplemental Fig. 5*B*). Hence, our data suggest that KLK8 is a keratinocyte-specific protease secreted during epidermal keratinocyte proliferation and abundantly secreted upon their terminal differentiation in culture (Fig. 7). However, not all co-localized epidermal KLKs evaluated were keratinocyte-specific. It is interesting to note that KLK7 was secreted by all epidermal cells investigated, although KLK5 and KLK8 were by far the most abundant secreted keratinocyte-specific KLKs (supplemental Fig. 5*A*).

KLK8 Is Expressed in a Free Form in Human Sweat and Non-palmoplantar Stratum Corneum

We collected, processed, and pooled normal human sweat and non-palmoplantar SC tissue extracts to investigate KLK8 expression and activity *ex vivo*. The final sweat and SC samples contained 8.0 and 3.5 mg of total protein, respectively. We detected KLK8 in both biological samples by Western blotting at a molecular mass similar to recombinant mat-KLK8 (~31 kDa) in a reduced SDS-PAGE. Processed forms of KLK8 in the sweat (~31 and 21 kDa) were also detected (Fig. 8). These results indicate that sweat and SC KLK8 is not covalently bound to an endogenous serine protease inhibitor. Whether the free form of sweat and SC KLK8 is catalytically active or inactive (mat-KLK8 or pro-KLK8) cannot be determined by expression analysis with Western blotting and requires specific activity-based probe analysis, as we describe below.

KLK8 Is Catalytically Active in Human Sweat and Non-palmoplantar Stratum Corneum

We sought to investigate KLK8 catalytic activity using an *ex vivo* skin model and recombinant mat-KLK8 as a positive control. We first confirmed the co-expression of multiple KLKs in sweat and SC epidermal extracts. According to our KLK-specific ELISA results, the pooled sweat sample contained 172 ng of KLK8/mg of total protein, 35 ng of KLK11/mg of total protein, and 2.2 ng of KLK5/mg of total protein. On the other hand, the pooled SC epidermal extract contained 28 ng of KLK8/mg of total protein, 63 ng of KLK11/mg of total protein, and 210 ng of KLK5/mg of total protein. Hence, we detected 78-fold higher concentration of KLK8 compared with KLK5 in sweat, and 7.5-fold lower concentration of KLK8 compared with KLK5 in the stratum corneum extracts. KLK11 was in the middle range between KLK5 and KLK8, as indicated above.

To detect KLK8 activity specifically, and no other KLK or serine protease activity, we immunocaptured KLK8 and tested its ability to cleave fluorogenic VPR-AMC substrate at different pH levels. The principle of the KLK8 immunocapture-activity assay we developed for this purpose is shown in Fig. 9*A*. We validated first that the monoclonal KLK8 antibody we used to coat the plate was a non-neutralizing antibody. We then performed a series of optimization steps using active recombinant mat-KLK8 protein. The sensitivity of the KLK8 immunocapture assay was optimized to detect a concentration-dependent increase in activity when an increased amount of active recombinant mat-KLK8 was loaded into KLK8-Ab-coated wells (supplemental Fig. 6). Assay specificity was also confirmed upon detecting no activity as a result of loading active KLK5 into wells coated with KLK8 antibody.

Approximately 40 ng of sweat KLK8, 4 ng of SC KLK8, and 250 ng of mat-KLK8 as well as 10× diluted samples of each were loaded in triplicate wells in the same 96-well plate coated with KLK8 antibody. We demonstrated a concentration- and time-dependent increase in AMC fluorescence emission in the nondiluted (1×) and (10×) diluted sweat and SC samples, confirming KLK8 activity in normal human skin surface (Fig. 9, *B* and *C*). The immunocaptured recombinant mat-KLK80 positive control reached saturation quicker than the immunocaptured sweat and SC KLK8, as expected, because of loading a significantly higher amount into the wells (5–10-fold higher than sweat-KLK8 and SC-KLK8). Immunocaptured SC and sweat KLK8 displayed optimal activity at pH 8.5 (Fig. 9, *B* and *C*) and retained lower, yet significant, activity at pH 5.0 (Fig. 9*D*). Hence, we elucidated KLK8 activity in the upper skin surface within the normal physiological pH gradient of human stratum corneum.

We also investigated if sweat and SC KLK8 contains some inactive pro-KLK8 proportion that can be activated by exogenous KLK5 or lysyl endopeptidase. Our results indicate that the majority of sweat and SC KLK8 was catalytically active (Fig. 10, *A* and *B*). These results, combined with our immunodetection of KLK5 in the same sweat and SC samples, suggest that KLK5 may have already activated a large proportion of sweat and SC KLK8. When recombinant pro-KLK8 was incubated with active KLK5 (1:100 molar ratio) or lysyl endopeptidase (1:1000 molar ratio), and immunocaptured as a positive control in the same KLK8 antibody-coated plate, we detected pro-KLK8 activation by both proteases (Fig. 10*C*).

DISCUSSION

We sought in this study to investigate KLK8 activity, regulation, and downstream targets to support its potential functional involvement in a proteolytic activation cascade regulating skin desquamation and antimicrobial defense. We previously described that multiple KLKs are co-localized in human epidermis and sweat and noted particularly an abundant expression of KLK8 (21). KLK8 is transported and exocytosed by lamellar granules into the stratum granulosum/stra-

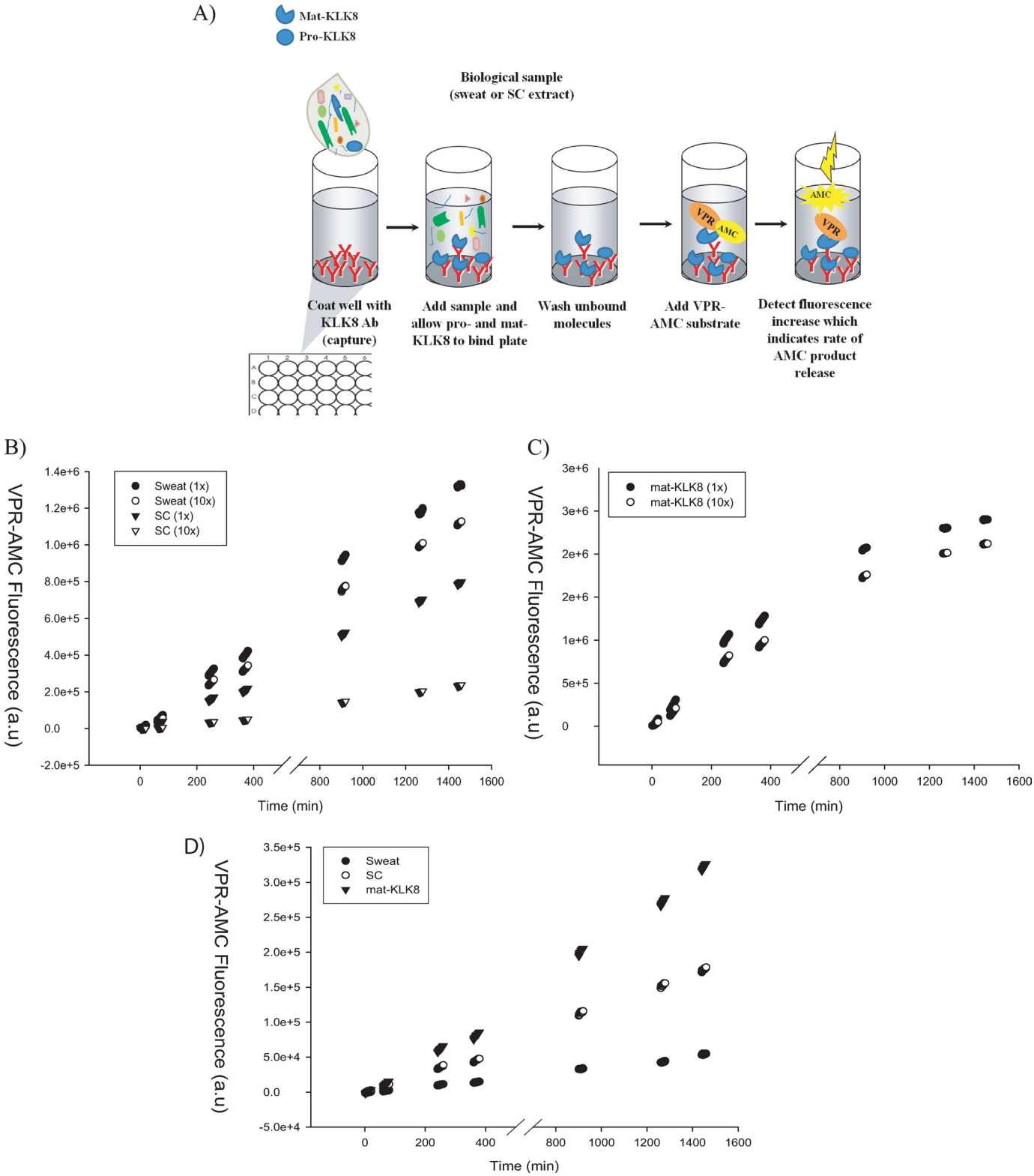

FIGURE 9. **Immunocapture of KLK8 activity in normal human sweat and non-palmoplantar stratum corneum *ex vivo*.** *A,* schematic representation of the principle of the KLK8-specific immunocapture activity assay. KLK8 is immunocaptured using a specific non-neutralizing monoclonal antibody. Potential nonspecific binding of other protease contaminants is eliminated through a series of stringent washes. The activity of the immobilized sweat or SC KLK8 is measured by monitoring fluorescence emission of VPR-AMC substrate compared with no-enzyme background control. *B,* time and concentration-dependent activity of immunocaptured sweat and SC KLK8 monitored in real time for a total of 24 h at 37 °C and pH 8.5. *C,* time- and concentration-dependent activity of immunocaptured recombinant mat-KLK8 activity as a positive control monitored in the same plate in real time for a total of 24 h at 37 °C and pH 8.5. *D,* time-dependent activity of the (1×) immunocaptured sweat, SC, and recombinant mat-KLK8 monitored in the same plate in real time for a total of 24 h at 37 °C at pH 5.0.

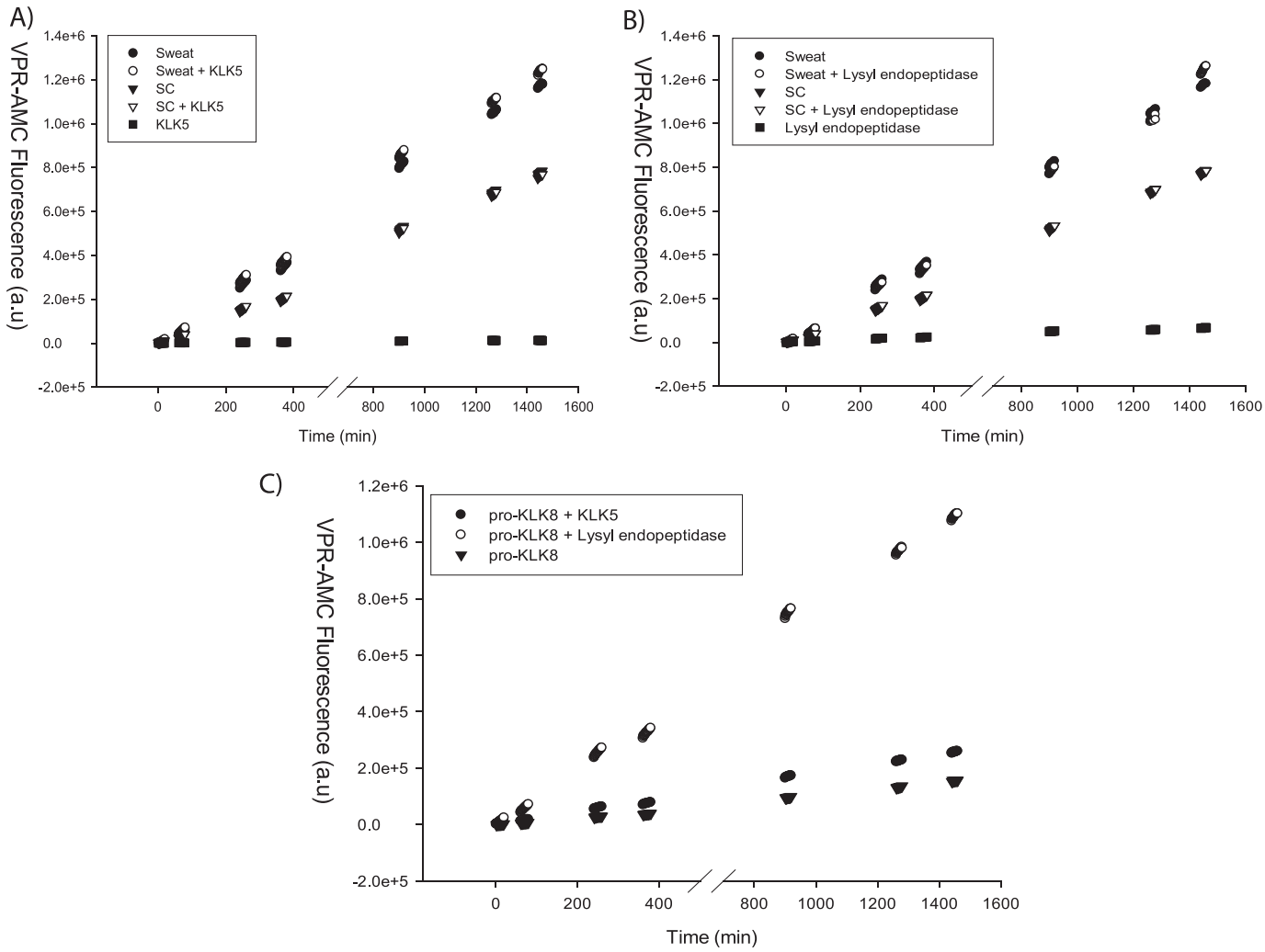

FIGURE 10. **Majority of sweat and SC KLK8 is catalytically active.** No significant increase in sweat and SC KLK8 activity was detected upon adding exogenous active KLK5 (*A*) or active lysyl endopeptidase (*B*) to the samples prior to performing KLK8 immunocapture-activity assays, compared with the immunocaptured recombinant pro-KLK8 positive control (*C*). The KLK5 and lysyl endopeptidase reaction rate was zero (slope of the FU/min graph), ensuring assay specificity.

tum corneum interface (49) and is thus likely activated in the SC extracellular space to play a role in SC barrier functions. Once activated, KLK8 activity is possibly regulated by many of the factors that control SC barrier integrity, such as epidermal pH and calcium ion gradients as well as endogenous serine protease/serine protease inhibitors. Here, we produced recombinant KLK8 in its precursor (pro-KL8) and active (mat-KLK8) forms and investigated a potential SC cascade-mediated role of KLK8 by examining *in vitro* its following potential: 1) to be regulated by pH and ions; 2) to be activated by co-localized serine proteases; 3) to be inhibited by co-localized serine protease inhibitors; 3) to activate co-localized pro-KLKs; and 4) to target co-localized LL-37 antimicrobial peptide activation.

Our results showed that recombinant KLK8 activity is pH-dependent, because it displayed maximal activity at an alkali pH of 8.5 and retained lower activity at pH 5. This suggests a role for KLK8 in human SC barrier where the pH decreases from 7.5 to 5 at the uppermost surface. Although the alkaline pH (where KLK8 activity is optimal) occurs in lower SC, it is possible that less active enzyme is present where the majority is in a latent pro-KLK8 form or is bound to endogenous inhibitors. More active enzyme may be present in the upper SC as a result of pro-KLK8 activation, being freed of a potential inhibitor, and/or the calcium ion gradient shift. Our studies indicate that KLK8 activity is enhanced by calcium and to a lesser degree by magnesium, two ions known to have higher concentrations in uppermost SC compared with lower layers. Interestingly, topical application of 10 mM $MgCl_2$ and $CaCl_2$ was shown to accelerate mouse skin barrier recovery after acute chemical disruptions (50). It is possible that magnesium and calcium ions influence barrier recovery via their activation of serine proteases such as KLK8. This possibility requires further investigation.

Because Zn^{2+} levels in human sweat (51) and in the skin of mammals may reach the millimolar range (52), this ion could be an important regulator of KLK8 activity in the skin. We showed that zinc ions, within physiological range, attenuate KLK8 activity. Zinc had a significantly lower inhibitory effect on KLK8 activity compared with other active epidermal KLKs, as 1:10 molar ratio of KLK to zinc ions resulted in 97.5 and 95% inhibition of KLK5 and KLK14 activity (30, 31), respectively, compared with 0% inhibition of KLK8. This suggests a

possibly different binding mode of zinc to KLK8 structure. However, the crystal structure of human KLK8 has not been resolved to date, and the mechanisms of zinc or calcium binding remain unknown.

Another important mode of regulating a protease irreversible cleavage of substrates is its pro-zymogen activation to generate the mature active form. We examined the ability of recombinant pro-KLK8 to be activated by epidermal trypsin-like serine proteases. Akin to pro-KLK8, the pro-enzymes of KLK7 and -14 require cleavage after lysine for activation. Pro-KLK7 and pro-KLK14 are activated by KLK5 in the human epidermis (11). Given that KLK5 is active in human SC as a result of autoactivation, we suspected that it activates pro-KLK8 in the deepest layers of the SC at the close-to-neutral pH. Our results show slow activation of pro-KLK8 by KLK5 within a day at room temperature at 10:1 molar ratio. This slow activation is similar to previous reports of KLK5 activation of pro-KLK7 (11), which may be important in normal skin physiology where SC layers get renewed every 2–4 weeks (53). Our *in vitro* results suggest that pro-KLK8 does not undergo autoactivation or activation by KLK1 but that it is activated slowly by KLK5 and rapidly by lysyl endopeptidase. Lysyl endopeptidase was a better activator of pro-KLK8 due to it specific cleavage after lysine residues. Hence, we put forward the lysine-specific enteropeptidase, discovered recently in human skin granular layer (54), as a potent potential endogenous activator of pro-KLK8.

KLK8 activity was not inhibited by any of the currently known endogenous epidermal inhibitors (LEKTI domains, SLPI, or elafin) in our study. Mat-KLK8 *in vitro* activity is inhibited by general serine protease inhibitors such as α_2-antiplasmin, aprotinin, protein C inhibitor, chymostatin, and to a low extent by soybean trypsin inhibitor. Unlike KLK5 and KLK14, α_1-antitrypsin does not inhibit mat-KLK8 activity at all (55). The P1-Arg preference of KLK8 and the presence of P1-Arg in α_2-antiplasmin and P1-Met in α_1-antitrypsin in these serpins may explain their different inhibitory potencies toward KLK8. Perhaps more interesting from a dermatological perspective is the finding that unlike epidermal KLK5–7, -13, and -14, and similar only to KLK1, KLK8 was not inhibited by any of the LEKTI domains implicated in the devastating skin disease, Netherton syndrome (40, 56). KLK8 activity was also recently shown to be completely unaffected by the new epidermal LEKTI inhibitors encoded by *SPINK6* and *SPINK9*, even though they inhibit KLK5, -7, and -14 (57–59). We demonstrated here that KLK8 activity could be inhibited by autocleavage after a solvent-exposed Arg^{164} in its computed tertiary structure, which was not previously reported. It is plausible that active co-localized trypsin-like KLKs, such as KLK14, may degrade KLK8 after Arg^{164} and reduce its activity. However, this possibility requires further assessment.

A recent study described KLK8 as a desquamatory enzyme that regulates the degradation of corneodesmosome through the actions of other kallikreins, in normal and barrier-disrupted mouse epidermis (29). KLK5 has not been detected in mouse epidermis to date. However, in human epidermis KLK5 is an active protease, which acts as an activator of pro-KLK8 zymogen as we showed here. We thus investigated the possibility that active KLK8 may target activation of pro-KLK11, which is also not yet detected in mouse epidermis but has been detected in human epidermis and sweat with unknown activators and undemonstrated activity/functionality to date. We elucidated KLK8 ability to activate pro-KLK11 *in vitro* using full recombinant KLK proteins that retain their native tertiary structure. KLK8 was also able to activate pro-KLK1 *in vitro*. Tissue kallikrein (KLK1) is active in human sweat (38), and our study is the first to identify a possible endogenous protease activator of KLK1 in sweat. Our results agree with the pro-KLK8 peptide activation findings by Yoon *et al.* (12), except for the fact that we did not detect activation of pro-KLK8 protein by active recombinant KLK1 protein. Overall, our data implicate KLK5 as an activation initiator and KLK8 as an upstream activator of KLK1 and KLK11 in an SC and sweat activation cascade.

SC serine proteases can also target LL-37 antimicrobial peptide processing in human skin to generate shorter antimicrobial peptides that are active against *Staphylococcus aureus* (14). We demonstrated the ability of KLK8 to process LL-37 synthetic peptide *in vitro*, leading to the formation of active KS-30, LL-29, and LL-23 antimicrobial peptides by trypsin-like cleavage. Yamasaki *et al.* (14) previously showed that trypsin-like KLK5 and chymotrypsin-like KLK7 are responsible for LL-37 processing in human skin surface, although other yet unknown serine proteases may be equally important in this process. Our *in vitro* data suggest KLK8 as a new potential regulator of LL-37 antimicrobial activity in human skin and sweat.

We showed here that chymostatin inhibits KLK8 activity, and we previously demonstrated that this chymotrypsin-like inhibitor is a better inhibitor of KLK8 than the trypsin-like inhibitor, leupeptin, with an IC_{50} of 8 μM compared with 66 μM, respectively (60). Epidermal KLK5 and KLK14 trypsin-like activity is efficiently inhibited by leupeptin but not by chymostatin (11). Interestingly, Yamasaki *et al.* (14) detected 80% reduction in skin surface serine protease activity by chymostatin and a minor reduction by leupeptin and suggested accordingly that the chymotrypsin-like KLK7 is a more potent enzyme than trypsin-like KLKs in human skin surface. Our data lead us to infer that trypsin-like KLK8 was present in the skin samples tested by Yamasaki *et al.* (14), contributing to the major serine protease activity inhibited by chymostatin and leading to LL-37 antimicrobial peptide trypsin-like processing. Furthermore, our detection of enhanced KLK8 *in vitro* expression and activity as a result of calcium induction of terminal keratinocyte differentiation and of pro-KLK8 activation by KLK5 and lysyl endopeptidase also suggested that KLK8 is active in uppermost epidermis.

We aimed to elucidate KLK8 activity in non-palmoplantar stratum corneum and sweat *ex vivo* by a KLK8-specific immunocapture activity assay using fluorogenic VPR-AMC substrate. This method allowed us to identify KLK8 serine protease activity in human epidermis and sweat for the first time, thus supporting our *in vitro* findings. The majority of SC and sweat KLK8 was present in a catalytically active form, displaying optimal activity at pH 8.5 and retaining activity at pH 5, similar to recombinant KLK8. Soap-treated, inflamed atopic

dermatitis and scaly psoriatic skins show alkali to neutral pH near optimum KLK8 activity (61). Hence, KLK8 hyperactivity in these conditions may contribute to their dry, flared-up, and inflamed symptoms, which remains to be studied.

To date, few active serine proteases were demonstrated in human sweat, including tissue kallikrein (KLK1) and kininase II (38). In the SC, kallikrein-related peptidase 5, 7, and 14 are the only described active serine proteases (11). Herein, we elucidated the presence of KLK8 as an active serine protease in human sweat and non-palmoplantar stratum corneum, raising its potential functional involvement in skin desquamation and antimicrobial proteolytic cascades. We identified the substrate specificity as well as potential endogenous activators and targets of this new active epidermal protease. As mentioned above, none of the currently known endogenous serine protease inhibitors exert an effect on KLK8 activity. Thus, KLK8 activity may affect the serine protease/serine protease inhibitor balance in normal human epidermis and skin diseases. Further understanding of the "unique" inhibition mechanism of KLK8 is needed for the development of KLK8 activity-based probing tools to study its function *in vivo* and for the development of KLK8-specific inhibitors as potential skin care and disease drug agents.

Acknowledgments—We thank Denitza Roudeva and Ioannis Prassas for their expertise and critical reading of this manuscript. We are grateful to Antoninus Soosaipillai for excellent laboratory technical assistance.

REFERENCES

1. Candi, E., Schmidt, R., and Melino, G. (2005) *Nat. Rev. Mol. Cell Biol.* **6,** 328–340
2. Eissa, A., and Diamandis, E. P. (2008) *Biol. Chem.* **389,** 669–680
3. Borgoño, C. A., and Diamandis, E. P. (2004) *Nat. Rev. Cancer* **4,** 876–890
4. Yousef, G. M., and Diamandis, E. P. (2000) *Genomics* **65,** 184–194
5. Yousef, G. M., and Diamandis, E. P. (2001) *Endocr. Rev.* **22,** 184–204
6. Brattsand, M., and Egelrud, T. (1999) *J. Biol. Chem.* **274,** 30033–30040
7. Egelrud, T., and Lundström, A. (1991) *Arch. Dermatol. Res.* **283,** 108–112
8. Stefansson, K., Brattsand, M., Ny, A., Glas, B., and Egelrud, T. (2006) *Biol. Chem.* **387,** 761–768
9. Egelrud, T., Hofer, P. A., and Lundström, A. (1988) *Acta Derm. Venereol.* **68,** 93–97
10. Lundström, A., and Egelrud, T. (1991) *Acta Derm. Venereol.* **71,** 471–474
11. Brattsand, M., Stefansson, K., Lundh, C., Haasum, Y., and Egelrud, T. (2005) *J. Invest. Dermatol.* **124,** 198–203
12. Yoon, H., Laxmikanthan, G., Lee, J., Blaber, S. I., Rodriguez, A., Kogot, J. M., Scarisbrick, I. A., and Blaber, M. (2007) *J. Biol. Chem.* **282,** 31852–31864
13. Lundström, A., Serre, G., Haftek, M., and Egelrud, T. (1994) *Arch. Dermatol. Res.* **286,** 369–375
14. Yamasaki, K., Schauber, J., Coda, A., Lin, H., Dorschner, R. A., Schechter, N. M., Bonnart, C., Descargues, P., Hovnanian, A., and Gallo, R. L. (2006) *FASEB J.* **20,** 2068–2080
15. Komatsu, N., Saijoh, K., Kuk, C., Shirasaki, F., Takehara, K., and Diamandis, E. P. (2007) *Br. J. Dermatol.* **156,** 875–883
16. Yamasaki, K., Di Nardo, A., Bardan, A., Murakami, M., Ohtake, T., Coda, A., Dorschner, R. A., Bonnart, C., Descargues, P., Hovnanian, A., Morhenn, V. B., and Gallo, R. L. (2007) *Nat. Med.* **13,** 975–980
17. Komatsu, N., Saijoh, K., Kuk, C., Liu, A. C., Khan, S., Shirasaki, F., Takehara, K., and Diamandis, E. P. (2007) *Exp. Dermatol.* **16,** 513–519
18. Briot, A., Deraison, C., Lacroix, M., Bonnart, C., Robin, A., Besson, C., Dubus, P., and Hovnanian, A. (2009) *J. Exp. Med.* **206,** 1135–1147
19. Komatsu, N., Takata, M., Otsuki, N., Ohka, R., Amano, O., Takehara, K., and Saijoh, K. (2002) *J. Invest. Dermatol.* **118,** 436–443
20. Komatsu, N., Saijoh, K., Toyama, T., Ohka, R., Otsuki, N., Hussack, G., Takehara, K., and Diamandis, E. P. (2005) *Br. J. Dermatol.* **153,** 274–281
21. Komatsu, N., Tsai, B., Sidiropoulos, M., Saijoh, K., Levesque, M. A., Takehara, K., and Diamandis, E. P. (2006) *J. Invest. Dermatol.* **126,** 925–929
22. Yoshida, S., Taniguchi, M., Hirata, A., and Shiosaka, S. (1998) *Gene* **213,** 9–16
23. Okabe, A., Momota, Y., Yoshida, S., Hirata, A., Ito, J., Nishino, H., and Shiosaka, S. (1996) *Brain Res.* **728,** 116–120
24. Inoue, N., Kuwae, K., Ishida-Yamamoto, A., Iizuka, H., Shibata, M., Yoshida, S., Kato, K., and Shiosaka, S. (1998) *J. Invest. Dermatol.* **110,** 923–931
25. Kitayoshi, H., Inoue, N., Kuwae, K., Chen, Z. L., Sato, H., Ohta, T., Hosokawa, K., Itami, S., Yoshikawa, K., Yoshida, S., and Shiosaka, S. (1999) *Arch. Dermatol. Res.* **291,** 333–338
26. Kirihara, T., Matsumoto-Miyai, K., Nakamura, Y., Sadayama, T., Yoshida, S., and Shiosaka, S. (2003) *Br. J. Dermatol.* **149,** 700–706
27. Kuwae, K., Matsumoto-Miyai, K., Yoshida, S., Sadayama, T., Yoshikawa, K., Hosokawa, K., and Shiosaka, S. (2002) *Mol. Pathol.* **55,** 235–241
28. Komatsu, N., Suga, Y., Saijoh, K., Liu, A. C., Khan, S., Mizuno, Y., Ikeda, S., Wu, H. K., Jayakumar, A., Clayman, G. L., Shirasaki, F., Takehara, K., and Diamandis, E. P. (2006) *J. Invest. Dermatol.* **126,** 2338–2342
29. Kishibe, M., Bando, Y., Terayama, R., Namikawa, K., Takahashi, H., Hashimoto, Y., Ishida-Yamamoto, A., Jiang, Y. P., Mitrovic, B., Perez, D., Iizuka, H., and Yoshida, S. (2007) *J. Biol. Chem.* **282,** 5834–5841
30. Michael, I. P., Sotiropoulou, G., Pampalakis, G., Magklara, A., Ghosh, M., Wasney, G., and Diamandis, E. P. (2005) *J. Biol. Chem.* **280,** 14628–14635
31. Borgoño, C. A., Michael, I. P., Shaw, J. L., Luo, L. Y., Ghosh, M. C., Soosaipillai, A., Grass, L., Katsaros, D., and Diamandis, E. P. (2007) *J. Biol. Chem.* **282,** 2405–2422
32. Luo, L. Y., Shan, S. J., Elliott, M. B., Soosaipillai, A., and Diamandis, E. P. (2006) *Clin. Cancer Res.* **12,** 742–750
33. Emami, N., and Diamandis, E. P. (2008) *J. Biol. Chem.* **283,** 3031–3041
34. Jayakumar, A., Kang, Y., Henderson, Y., Mitsudo, K., Liu, X., Briggs, K., Wang, M., Frederick, M. J., El-Naggar, A. K., Bebök, Z., and Clayman, G. L. (2005) *Arch. Biochem. Biophys.* **435,** 89–102
35. Jayakumar, A., Kang, Y., Mitsudo, K., Henderson, Y., Frederick, M. J., Wang, M., El-Naggar, A. K., Marx, U. C., Briggs, K., and Clayman, G. L. (2004) *Protein Expr. Purif.* **35,** 93–101
36. Komatsu, N., Saijoh, K., Sidiropoulos, M., Tsai, B., Levesque, M. A., Elliott, M. B., Takehara, K., and Diamandis, E. P. (2005) *J. Invest. Dermatol.* **125,** 1182–1189
37. Bernard, D., Méhul, B., Thomas-Collignon, A., Simonetti, L., Remy, V., Bernard, M. A., and Schmidt, R. (2003) *J. Invest. Dermatol.* **120,** 592–600
38. Hibino, T., Takemura, T., and Sato, K. (1994) *J. Invest. Dermatol.* **102,** 214–220
39. Borgoño, C. A., Michael, I. P., Komatsu, N., Jayakumar, A., Kapadia, R., Clayman, G. L., Sotiropoulou, G., and Diamandis, E. P. (2007) *J. Biol. Chem.* **282,** 3640–3652
40. Deraison, C., Bonnart, C., Lopez, F., Besson, C., Robinson, R., Jayakumar, A., Wagberg, F., Brattsand, M., Hachem, J. P., Leonardsson, G., and Hovnanian, A. (2007) *Mol. Biol. Cell* **18,** 3607–3619
41. Descargues, P., Deraison, C., Bonnart, C., Kreft, M., Kishibe, M., Ishida-Yamamoto, A., Elias, P., Barrandon, Y., Zambruno, G., Sonnenberg, A., and Hovnanian, A. (2005) *Nat. Genet.* **37,** 56–65
42. Ohler, A., Debela, M., Wagner, S., Magdolen, V., and Becker-Pauly, C. (2010) *Biol. Chem.* **391,** 455–460
43. Gallo, R. L., Murakami, M., Ohtake, T., and Zaiou, M. (2002) *J. Allergy Clin. Immunol.* **110,** 823–831
44. Lee, P. H., Ohtake, T., Zaiou, M., Murakami, M., Rudisill, J. A., Lin, K. H., and Gallo, R. L. (2005) *Proc. Natl. Acad. Sci. U.S.A.* **102,**

3750–3755
45. Murakami, M., Ohtake, T., Dorschner, R. A., Schittek, B., Garbe, C., and Gallo, R. L. (2002) *J. Invest. Dermatol.* **119,** 1090–1095
46. Hennings, H., and Holbrook, K. A. (1983) *Exp. Cell Res.* **143,** 127–142
47. Menon, G. K., and Elias, P. M. (1991) *Arch. Dermatol.* **127,** 57–63
48. Menon, G. K., Elias, P. M., and Feingold, K. R. (1994) *Br. J. Dermatol.* **130,** 139–147
49. Ishida-Yamamoto, A., Simon, M., Kishibe, M., Miyauchi, Y., Takahashi, H., Yoshida, S., O'Brien, T. J., Serre, G., and Iizuka, H. (2004) *J. Invest. Dermatol.* **122,** 1137–1144
50. Denda, M., Katagiri, C., Hirao, T., Maruyama, N., and Takahashi, M. (1999) *Arch. Dermatol. Res.* **291,** 560–563
51. Crew, A., Cowell, D. C., and Hart, J. P. (2008) *Talanta* **75,** 1221–1226
52. Nitzan, Y. B., Sekler, I., and Silverman, W. F. (2004) *J. Histochem. Cytochem.* **52,** 529–539
53. Milstone, L. M. (2004) *J. Dermatol. Sci.* **36,** 131–140
54. Nakanishi, J., Yamamoto, M., Koyama, J., Sato, J., and Hibino, T. (2010) *J. Invest. Dermatol.* **130,** 944–952
55. Luo, L. Y., and Jiang, W. (2006) *Biol. Chem.* **387,** 813–816
56. Descargues, P., Deraison, C., Prost, C., Fraitag, S., Mazereeuw-Hautier, J., D'Alessio, M., Ishida-Yamamoto, A., Bodemer, C., Zambruno, G., and Hovnanian, A. (2006) *J. Invest. Dermatol.* **126,** 1622–1632
57. Brattsand, M., Stefansson, K., Hubiche, T., Nilsson, S. K., and Egelrud, T. (2009) *J. Invest. Dermatol.* **129,** 1656–1665
58. Hachem, J. P., Wagberg, F., Schmuth, M., Crumrine, D., Lissens, W., Jayakumar, A., Houben, E., Mauro, T. M., Leonardsson, G., Brattsand, M., Egelrud, T., Roseeuw, D., Clayman, G. L., Feingold, K. R., Williams, M. L., and Elias, P. M. (2006) *J. Invest. Dermatol.* **126,** 1609–1621
59. Meyer-Hoffert, U., Wu, Z., Kantyka, T., Fischer, J., Latendorf, T., Hansmann, B., Bartels, J., He, Y., Gläser, R., and Schröder, J. M. (2010) *J. Biol. Chem.* **285,** 32174–32181
60. Kishi, T., Cloutier, S. M., Kündig, C., Deperthes, D., and Diamandis, E. P. (2006) *Biol. Chem.* **387,** 723–731
61. Hachem, J. P., Roelandt, T., Schürer, N., Pu, X., Fluhr, J., Giddelo, C., Man, M. Q., Crumrine, D., Roseeuw, D., Feingold, K. R., Mauro, T., and Elias, P. M. (2010) *J. Invest. Dermatol.* **130,** 500–510